Thesis

CHARACTERISATION OF CARDIAC FUNCTION AND STRUCTURE IN AN ATHEROSCLEROSIS PRONE MOUSE MODEL OF OBESITY AND TYPE 2 DIABETES

submitted by

Franz Cichocki

In partial fulfillment of the requirements for the degree of

Doktor der gesamten Heilkunde

(Dr. med. univ.)

at the

Medical University of Graz

executed at the

University Department of Internal Medicine

Division of Cardiology, University Heart Center Graz

Under the supevision of

Assoz. Prof. Priv.-Doz. Dr Bugger, Heiko

Byrne, Nikole Ph.D

Graz, 02.09.24

1 Declaration of Academic Integrity

I hereby confirm that the present diploma thesis is the result of my own independent scholarly work. I also confirm that in all cases, where material from the work of others (in books, articles, essays, dissertations, and on the internet) is acknowledged, quotations and paraphrases are clearly indicated. No material other than that cited in the reference list has been used. I have read and understood the Medical University's regulations and procedures concerning plagiarism.

Graz, am 02.09.2024 Franz Cichocki m.p.

2 Acknowledgments

First of all, I would like to thank Assoz. Prof. Priv.-Doz. Dr. Heiko Bugger for introducing me to the world of medical science. He not only provided this thesis' topic but also gave me the opportunity to learn established laboratory techniques used in cardiovascular research under his supervision in his research group. Beyond that, in our many conversations, he inspired me in my ideas about my own medical future.

Next, I would like to thank Nikole Byrne Phd., who always supported me with advice of any kind in my daily work in the lab, helped me to learn the techniques used to acquire this thesis data and provided good comments on the draft.

Finally, I would like to thank the rest of the "Cardiac Energetics" group Katharina, Ivan, Thomas & Carolin who helped me on my way in realizing my experiments but also made work in the lab enjoyable.

I would also like to take the possibility to like to thank my family who supported me throughout my studies. My mother who always listened to whatever was on my mind and my father who gave me the persistence I needed to work hard for my exams. They never questioned my ways of doing my studies but always believed in me.

Last but not least, I would like to thank my grandfather Dr. med. univ. Gerhard Pratl to whom I would like to dedicate this work. Since I was a child he has shown me his way of being a doctor and inspired me in how I would like to be as a doctor one day.

3 Zusammenfassung

Adipositas und Typ-2-Diabetes mellitus (T2DM) sind allgemein bekannte Risikofaktoren für kardiovaskuläre Erkrankungen welche von leichter diastolischer Dysfunktion, bis zu Herzversagen (HF) reichen können. Tiermodelle für Adipositas und T2DM werden häufig zur Untersuchung der diastolischen Dysfunktion verwendet, aber nicht zur Untersuchung der Entwicklung von Atherosklerose. Um auch Atherosklerose zu untersuchen, braucht es ein Tiermodell mit einer hierfür prädisponierenden Mutation. So ist es möglich, den Beitrag der Atherosklerose und der vaskulären Dysfunktion zu untersuchen, die Menschen mit T2DM normalerweise ebenso entwickeln. Ziel dieser Studie war es, die Auswirkungen von Fettleibigkeit und T2DM auf die Herzfunktion und -struktur in einem Mausmodell zu untersuchen, das auch Atherosklerose entwickelt.

In unserer Studie wurden Ldlr$^{-/-}$ Mäuse 16 Wochen lang mit normalem Futter (n=10) oder mit sogenannter „westlicher Diät“ (WD; n=10) gefüttert, wobei Körpergewicht, Nahrungs- und Wasseraufnahme wöchentlich gemessen wurden. Nach 8 und 16 Wochen Futter bzw. oder WD-Ernährung wurden Glukosetoleranztests durchgeführt. Zur Messung der Herzfunktion und -struktur wurde eine Echokardiographie durchgeführt. Die Größe der Kardiomyozyten wurde mit der WGA-Färbung und der Anteil der kardialen Fibrose mit der Masson-Trichrom-Färbung bestimmt.

WD verursachte eine Zunahme des Körpergewichts im Verlauf der Studie und führte zu erhöhten Serumglukosewerten nach intravenöser Glukosegabe. Das HW/TL-Verhältnis war bei Mäusen, die mit WD gefüttert wurden, signifikant niedriger, was auf eine geringere Herzgröße trotz erhöhten Körpergewichts hindeutet. Die Kardiomyozytengröße unterschied sich nicht zwischen den Gruppen. Bei der Echokardiographie war die Ejection Fraction zwischen den Gruppen nicht unterschiedlich. Der diastolische Durchmesser und das diastolische Volumen waren vermindert, aber bei Normalisierung auf Herzgewicht waren diese Werte nicht mehr unterschiedlich. Im Gegensatz dazu war die Wanddicke zwischen den Gruppen unverändert, aber bei Normalisierung auf das Herzgewicht ergab sich eine deutlich erhöhte Wanddicke, was auf eine kardiale Hypertrophie hindeutet. Die E/A- und E/E'-Werte, die auf eine diastolische Dysfunktion hinweisen, wiesen niedrigere Mittelwerte auf, die jedoch statistisch nicht signifikant waren. Das auf das Körpergewicht normalisierte Herzzeitvolumen war bei mit WD gefütterten Mäusen deutlich niedriger. Bemerkenswert ist, dass die histologische Analyse des LV-Myokards trotz der erhöhten Wanddicke keinen wesentlichen Unterschied im Kollagengehalt des Herzens bei Mäusen, die mit WD gefüttert wurden, erkennen ließ.

Wir kommen zum Schluss, dass WD bei Ldlr$^{-/-}$ Mäusen charakteristische Merkmale des metabolischen Syndroms wie Fettleibigkeit und Insulinresistenz hervorruft. In diesem Tiermodel welche eine Schwächung der Herzfunktion durch Diät und Gewichtszunahme bedingt, kann WD ein hypertrophes kardiales Remodeling und möglicherweise eine diastolische Dysfunktion hervorrufen. Eine geringere Herzgröße kann die Herzleistung von fettleibigen Ldlr$^{-/-}$ Mäusen einschränken. Somit zeigt dieses zur Atherosklerose neigende Modell von Adipositas und T2DM Merkmale der diabetischen Kardiomyopathie, die auch in anderen Tiermodellen ohne Atherosklerose beobachtet wurden.

4 Abstract

4.1 Background

Obesity and Type 2 diabetes mellitus (T2DM) increase the risk for heart failure (HF), including diastolic dysfunction. While animal models of obesity and T2DM used for mechanistic research display diastolic dysfunction, these models usually lack development of atherosclerosis unless an atherosclerosis predisposing mutation has been included. Thus, these animal models do not allow to estimate the additional contribution of atherosclerosis and vascular dysfunction which however commonly develop in humans with T2DM. Thus, the aim of the current study was to investigate the effects of obesity and T2DM on cardiac function and structure in a mouse model that also develops atherosclerosis.

4.2 Methods

$Ldlr^{-/-}$ mice were fed either normal chow (n=10) or a western diet (WD; n=10) for 16 weeks. Body weight, food and water intake were measured on a weekly basis. Glucose tolerance tests were performed after 8 and 16 weeks of chow or WD feeding. Echocardiography was performed to measure cardiac function and structure. Cardiomyocyte size was evaluated using WGA staining, and fibrosis was evaluated using Masson's trichrome stain.

4.3 Results

WD led to a continuous increase in body weight over time and resulted in increased serum glucose values following intravenous glucose challenge. The mean values of HW/TL ratios were significantly lower in WD fed mice, indicating smaller heart size despite increased body weight. There was no difference in cardiomyocyte size between groups. Echocardiography revealed no difference in ejection fraction between groups. Diastolic diameter and volume were decreased, however when normalizing to HW, these values were not different anymore. Wall thickness remained unchanged between groups, but normalization to HW resulted in significantly increased wall thickness, indicative of cardiac hypertrophy. E/A and E/E' values indicative of diastolic dysfunction showed lower mean values although not quite statistically significant. Cardiac output normalized to BW was markedly lower in WD fed mice. Histological analysis of LV myocardium did not reveal any major difference in cardiac collagen content despite increased wall thickness in WD fed mice.

4.4 Conclusion

WD induced characteristic traits of the metabolic syndrome such as obesity and insulin resistance in $Ldlr^{-/-}$ mice. Nevertheless, in this model, body weight-driven gain of heart weight may be attenuated whereas WD may induce hypertrophic cardiac remodeling and potentially diastolic dysfunction. Smaller heart size may limit cardiac output of obese $Ldlr^{-/-}$ mice. Thus, this atherosclerosis prone model of obesity and T2DM exhibits features of diabetic cardiomyopathy similar to those observed in other animal models that do not have atherosclerosis.

5 Publication

At the time of submission, this thesis has not been published.

6 Table of Contents

7 Table of Abbreviations

Table 1: Abbreviations

AB 1	Abelson interactor 1
Acyl CoA	Acyl Coenzyme A
AGES	Advanced Glycation Endproducts
AHA	American Heart Association
Ang II	Angiotensin II
ANOVA	Analysis of Variance
Apo E	Apolipoprotein E
ATP	Adenosine triphosphate
CAD	Coronary Artery Disease
cGMP	cyclic GMP
CMRI	Cardiac magnetic resonance imaging
CTGF	Connective tissue growth factor

DBP	Diastolic Blood Pressure
ddH_2O	Double-distilled water
Diabetes mellitus type 2	T2DM
DM	Diabetes mellitus
DMCMP	Diabetic cardiomyopathy Cardiomyopathy
ECM	Extracellular matrix
ER stress	Endoplasmatic reticulum stress
ESC	European Society of Cardiology
ETC	Lysosomal electron transport chain
Foxo	Fox o family transcription factors
GTT	Glucose Tolerance Test
H&E staining	Hematoxylin and eosin staining
HDL	High density lipoprotein
HF	Heart frequency
HFpEF	heart failure with preserved ejection fraction
HFrEF	Heart failure with reduced ejection fraction
IDL	Intermediate density lipoprotein
IGF1R	Insulin like growth factor 1 receptor
LDL	Low density lipoprotein
Ldlr$^{-/-}$ mouse	Low density lipoprotein receptor deficient mouse
LFPVDF	Low Fluorescence Polyvinylidene difluoride
LV	Left ventricular
LVEDVI	Left ventricular end diastolic volume index
LVEF	Left ventricular ejection fraction
LVH	Left ventricular hypertrophy
LVMI	Left ventricular mass index
miRNAS	Micro RNAs
MMPs	Matrix metalloproteinases
NaCl solution	Physiological saline solution
NO	Nitric oxide
NR	Nicotinamide riboside
NRF2	Nuclear factor erythroid 2-related factor 2
ObRb	Leptin or obesity receptor
OCT	Optimal Cutting Temperature Compound
PARP 1	Poly (ADP-ribose) polymerase 1
PFA	Paraformaldehyde
PSLAX	Peristernal long axis view
RNS	Reactic nitrogen species
ROS	Reactive oxidation species
SAX	Short axis view
sGC	soluble guanylate cyclase
SGK 1	Serine/threonine-protein kinase 1
SGLT 2	Sodium Glucose Transporter 2
Sirtuin	Silent mating type information regulation
SOD	Superoxide dismutase
SR	Sarcoplasmic reticulum
SRBI	Scavenger receptor class b, type I

T - test	Hypothesis test statistic
TGF-β	Transforming growth factor beta
TIMPS	tissue inhibitors of metalloproteinases
VLDL	Very low density lipoprotein
WD	Western Diet
WGA	Wheat germ agglutinin

8 Table of Figures

9 List of Tables

10 Diabetic Cardiomyopathy

10.1 Clinical perspective

Diabetic Cardiomyopathy is a rising disease worldwide with over 37.3 million adults that are diagnosed with diabetes mellitus only in the USA. Some studies claim more than 10% of patients diagnosed with diabetes mellitus also present with DbCM (Segar, et al., 2021) although the prevalence varies depending on the criteria used to classify this disease. The association of a connection between diabetes mellitus and increased heart disease, was confirmed by numerous epidemiological studies, most recently the Framingham Heart Study (Rutter et al.). However, what all epidemiological studies agree is that DbCM is more than a comorbidity to heart failure - in fact, a diagnosed diabetes mellitus is a known risk factor and a prerequisite for the diagnosis DbCM. (Dandamudi S, 2014)

This rising prevalence of DbCM may also be attributed to the development of enhanced diagnostic algorithms. Moreover, there is an increased clinical awareness of the crucial significance of heart failure especially with an enhanced focus on diastolic function as a disease. All these facts considered, the diagnostic progress in DbCM allows patients with diabetes mellitus to start treatment before symptoms of heart failure occur and modulate the disease to an acceptable level. (Ritchie & Dale, 2020)

Finally, it needs to be mentioned that, the European Society for Cardiology does not recognize the existence of DbCM in their guidelines in 2019. They explain this by saying that evidence that supports its existence mostly comes from experimental work and small observational studies. The guidelines do acknowledge, however, that the bidirectional relationship between heart failure and diabetes mellitus must be investigated further in studies. (Consentino, 2020) The American College of Cardiologists and the American Heart Association just recognize diabetes mellitus as a major risk factor for heart failure but do not mention DbCM as its own clinical entity. (Stewart, et al., 2020)

Diabetic Cardiomyopathy is a multifactorial disease that was first proposed by Lundbaek in 1954 (Lundbaek, 1954). He suggested that the myocardial dysfunction in his diabetes mellitus (DM) patients should be seen as a new clinical entity of a specific diabetes mellitus – related cardiomyopathy. (Seferović, 2015) In 1972 this was confirmed by Rubler who autopsied four cased with diabetic glomerulosclerosis and no known heart failure. (Rubler, 1972) Today the typical definition of DbCM consists of the structural and functional abnormalities of the myocardium in diabetic patients that have no coronary artery disease nor hypertension. (Miki, 2013) In other words, the characteristics of DbCM are the joint presence of diabetes mellitus, cardiac hypertrophy, and myocardial stiffness without hypertension, atherosclerosis, and coronary artery disease (CAD). (Aneja, 2008)

A problem facing clinicians today is that there are no guidelines for making the diagnosis of DbCM. The reason for that is a lack of universal consensus on an unanimous accepted definition of what pathologies DbCM consists. If defined most basically as heart failure with an existing diabetes mellitus it raises the question of when a is heart failing or how diabetes mellitus is defined. It is known that the progression of DbCM often begins with left ventricular (LV) diastolic dysfunction which mostly occurs long before clinically relevant LV systolic dysfunction affects a patient's daily life thus long before a heart is failing. As said,

diastolic dysfunction has an immense role in the progression of cardiac function in DbCM. The progression of clinical possibilities, made it possible to assess the diastolic function in all patients in a routine clinical examination. This was not usual practice up until recently. This shift is attributed to advanced imaging techniques e.g. echocardiography with better ultrasound machines. The graduation of DbCM can be done according to the degree of diastolic dysfunction assessed in echocardiography. However, up until today there is also no conscensus on an unanimous definition of diastolic heart failure that is universly accepted in the medical community. If DbCM stages are based on the degree of diastolic dysfunction the graduation is impossible if one cannot agree on a definition for diastolic dysfunction on its own. (Galderisi, 2005) The gold standard for diagnosing DbCM, however, still is cardiac magnetic resonance imaging. (Ritchie & Dale, 2020)

Most clinicians would see the diagnosis of DbCM as a combination of symptoms of heart failure, different clinical evaluations and tests. (Gazewood, 2017) At the moment the best way to in fact make the diagnosis DbCM is to detect functional and structural changes and exclude the possibility of other heart disease. (Miki, 2013)
In one of their reviews Miki et. al identify some of these diagnostic clues:

Table 2 Diagnostic Clues for DbCM

Structural changes:
LV hypertrophy assessed by two dimensional echocardiography or cardiac magnetic resonance imaging
Increased integrated backscatter in the LV (septal and posterior wall)
Late Gadolinium-enhancement of the myocardium in cardiac magnetic resonance imaging
Functional changes:
LV diastolic dysfunction assessed by pulsed Doppler echocardiography and tissue Doppler imaging
LV systolic dysfunction demonstrated by tissue Doppler imaging/strain imaging
Limited systolic and/or diastolic functional reserve assessed by exercise tissue Doppler imaging
Metabolic changes:
Reduced cardiac PCr/ATP detected by 31P-magnetic resonance spectroscopy
Elevated myocardial triglyceride content detected by 1H-magnetic resonance spectroscopy

They state that functional changes such as a left ventricular diastolic dysfunction detected by tissue Doppler imaging may be the earliest sign of a diabetes – induced left ventricular dysfunction. Furthermore, they propose the assessment of interstitial fibrosis by Gadolinium enhancement of cardiac MRI although it is not yet well established. Finally, they suggest a novel approach to the diagnosis by characterizing metabolic myocardial changes. This can be done by a special protocol of magnetic resonance spectroscopy by which reduced cardiac PCr/ATP can be detected by 31P-magnetic resonance spectroscopy. PCr/ATP ratio is an index of energy charge that seems to be reduced in the myocardium of diabetic patients. This is debated to be a clue for the development of DbCM. (Miki, 2013)

1H-magnetic resonance spectroscopy is a new diagnostic idea that targets the increase of myocardial triglyceride conctent, thus basically is myocardial steatosis. This again, is said to be associated with left ventricular dysfunction in diabetic patients. (McGavock, 2007)

Many basic research publications agree that systolic and diastolic dysfunction have been routed with changes in cardiac morphology that are unique to this disease. Hence, Ghanghong et al. suggest that DbCM should be based on pathophysiological not clinical changes. They propose, there should be an early, intermittent, and late stage of DbCM. This would confirm our clinical experience, as the difference between mild, moderate and severe DbCM patients can be huge. Symptoms can go on a spectrum from asymptomatic to severe. (Ghuanghong, 2015)

Summing up, what is missing however, are easy diagnostic criteria for everyday daily clinical use. Interestingly, there are hardly any discussed in guidelines or in the literature. Only Seferović et al. recently proposed some (Figure 1). (Seferovic, 2015)

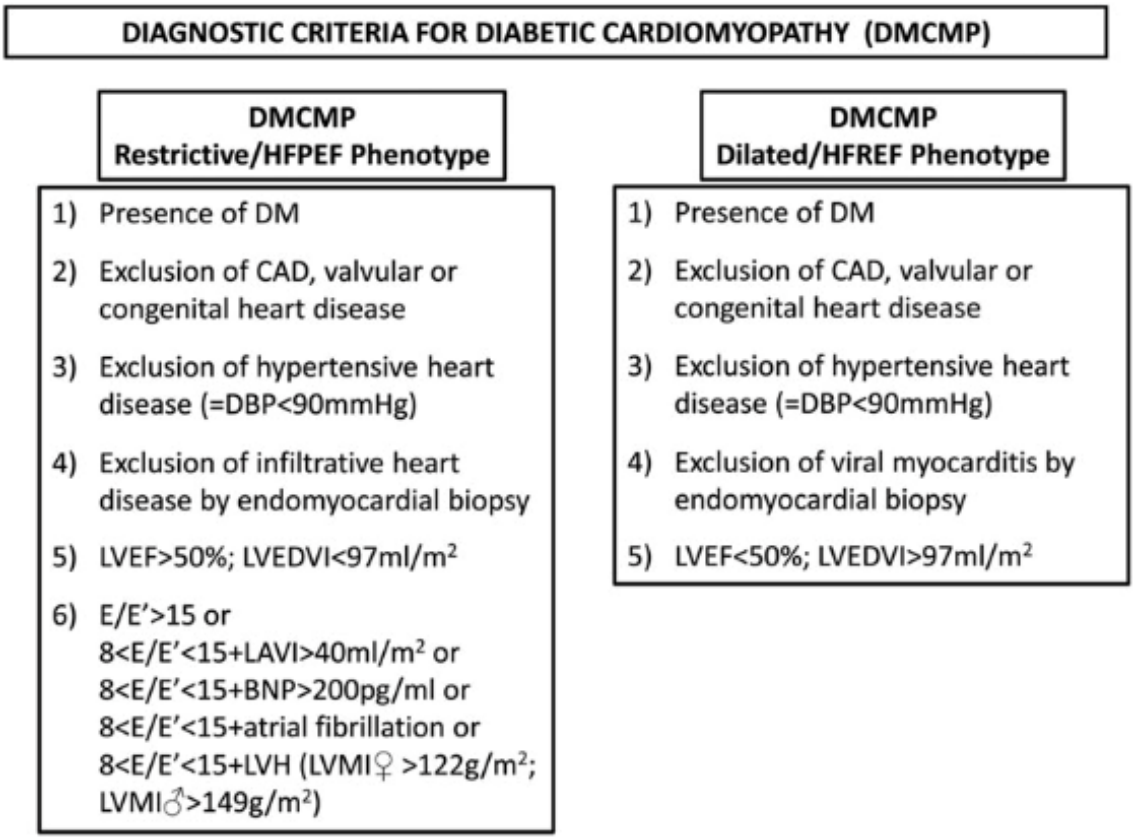

Figure 1: Diagnostic Criteria for Diabetic Cardiomyopathy

In the end stage, DbCM normally results in heart failure with preserved ejection fraction (HFpEF). However, some authors even argue that DbCM may result in systolic heart failure (HFrEF) which there is no evidence from prospective studies yet. (Hölscher, 2016)

10.2 Molecular Mechanisms

DbCM is a complex multi-aspect disease that is influenced by many molecular pathways. In a review trying to line out these molecular influences Tan et al. (Tan, 2020) claimed that the origin of the disease is impaired glucose and lipid metabolism, thereby increasing

cellular oxidative stress. ROS are then responsible for the activation of multiple inflammatory pathways. This way, micro and macro pathognomonic changes in DbCM such as cellular and extracellular injury, cardiac remodeling, and diastolic and systolic dysfunction occur.

Increased levels of glucose and metabolites, an upregulation of advanced glycation end products can affect cardiomyocytes and endothelial cells. (Brunvand, 2017) A metabolic shift in cardiomyocytes which causes fatty acid intake and β-oxidation to increase due to a lack of insulin or even insulin resistance in order to keep ATP production sufficiently. This process cannot be maintained β-oxidation is not made to metabolize all incoming fatty acid resulting in intracellular lipid accumulation and lipotoxicity. (Ramesh, 2022) This results in mitochondrial dysfunction which causes the generation of reactive oxygen species (ROS) and reactive nitrogen species (RNS) which enhance oxidative stress, endoreticulum stress and inhibit autophagy. (Kenny, 2019)

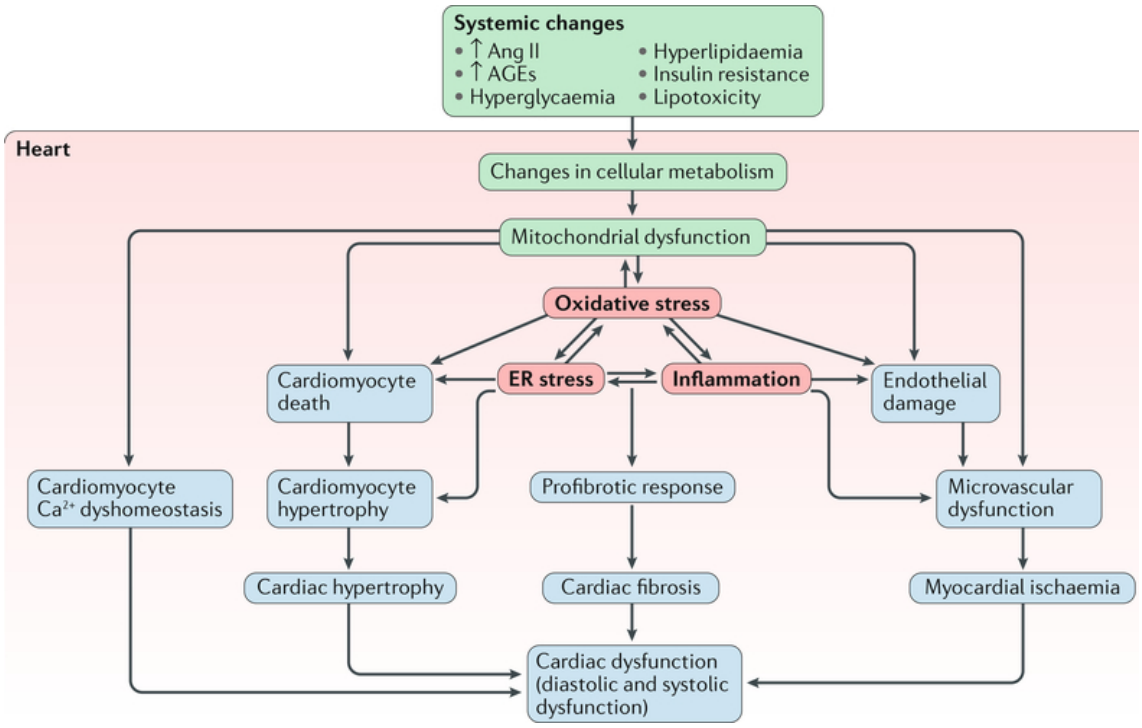

Figure 2: Mechanisms of Diabetic Cardiomyopathy

In Figure 2 one can see that cardiac oxidative stress is a central element in the pathophysiological progression of DbCM. Per definition this is an imbalance of the generation of free radicals and antioxidants. In DbCM it is reactive oxygen species (ROS) and reactive nitrogen species (RNS) that promote oxidative stress. (Cai, 2001) (Wilson, 2018) Furthermore, in the diabetic heart the antioxidants the body's natural protection are compromised thus also increase oxidative stress. (Nishikawa, 2000) (Tan Y. , 2011) Myocardial oxidative stress is promoted by the activation of cellular and mitochondrial NOX, which lead to the generation of superoxide and hydrogen peroxide. (Wilson, 2018) (Giacco, 2010) On the contrary it is the superoxide dismutases (SOD) that

are the body's defense by catalyzing the dismutation of superoxide radical into oxygen or hydrogen peroxide. (Fukai T, 2011)

Metabolic impaired glucose levels and their association with increased ROS may contribute to cardiomyocyte and endothelial cell apoptosis and necrosis in diabetic hearts. This may be due to the activation of the renin-angiotensin system. Discussed to be responsible for this apoptosis is the nuclear factor erythroid 2-related factor 2 (NRF2) which has shown to be a major regulator of myocardial oxidative stress and apoptosis. When knocked out in rodent studies apoptosis due to hyperglycemia ocurred more often. (Xiaoquing, 2008) Moreover, angiotensin II induced cardiomyopathy due to NRF2 deficiency happened more often in contrast to NRF2 overexpression where it declined due to resistance. (Xin, 2018) (Gu, 2016) Furthermore, angiotensin II also contributes to increased interstitial fibrosis. (Boudina, 2007) (Frustaci, 2000)

Cardiac hypertrophy, primarily left ventricular hypertrophy (LVH), is characterized by increased LV mass. LVH is usually caused by a complex interaction between several factors, such as hypertension, diabetes, metabolic syndrome, obesity, gender, ethnicity, and genetic and neurohumoral factors amongst others. A recent review by Murtaza et al. studied the impact of cardiac hypertrophy on the development of diastolic dysfunction. Reduced left ventricular compliance, impaired diastolic filling, and prolonged isovolumetric relaxation are associated with cardiac hypertrophy. All of these lead to an increase in left ventricular and left atrial filling pressures which makes them driving factors for the development of diastolic dysfunction. (Oktay, 2020) (Murtaza, 2019)

Cytokines, chemokines and exosomes secreted by inflammatory cells can influence cardiomyocyte hypertrophy and extra cellular matric (ECM) remodeling by promoting some myocardial processes. Factors such as hyperlipidemia, elevated angiotensin II levels and inflammation. They are upregulated by proinflammatory macrophages and lymphocytes which can secrete cytokines such as TNF, IL-6, IL-1β, interferon-γ and TGFβ that can induce or exacerbate cardiac injury, leading to further adverse remodeling. (Dinh, 2009) (Bajai, 2018). This hypothesis is supported by studies that inhibited the formation of T cells in the hearts of diabetic mice and saw a stop in the progression of cardiac fibrosis and LV dysfunction. (Laroumanie, 2014) (Nevers, 2015) Another explanation for cardiac hypertrophy is due to enhanced presence of reactive oxygen species (ROS) and reactive nitrogen species (RNS) there is less nitric oxide (NO). Reduced NO signaling in endothelial cells and cardiomyocytes increase cardiomyocyte hypertrophy and stiffness by decreasing soluble guanylate cyclase (sGC) activity and cyclic GMP (cGMP) content in the myocardium which is not protected by protein kinase G. This results in myocardial stiffness and cardiac hypertrophy. (Cruz, 2017) (Sorop, 2018) (Csabe, 2016) In a way this is where pathophysiological mechanisms of cardiac hypertrophy and cardiac fibrosis promote each other.

On a genetic level, there are many hypotheses on what is responsible for cardiac hypertrophy. One of them is, that it is due to altered miRNAs. miRNAs are short chains of 21-23 nucleotides, that have significant effects on the regulation of gene expression. In one of their publications, Tan et al. suggested that the suspected miRNA responsible for cardiac hypertrophy could be miR133a. They showed that miR133a is downregulated in

DbCM mice but its regulators MEF2A and MEF2C were increased in rodent models. MEF2A and MEF2C are modulated by serine/threonine – protein kinase 1 SGK1 and insulin growth factor 1 receptor IGF1R. Hence, they claim, it is SGK1 and IGF1R that are responsible for the hypertrophic effects. (Feng, 2010)

Increased fibrosis is often observed in DbCM. ECM homeostasis is normally regulated by two key factors metalloproteinases (MMPS) and tissue inhibitors of metalloproteinases (TIMPS) (Mishra, 2013) (Horn, 2015) For T2DM however, the situation is different. Advanced glycation end products (AGE) which result of proteins and lipids that are exposed to high glucose levels too long, crosslink ECM proteins and disturb the ECM degradation by MMPs. (Heerebeek, 2007) Specifically, a systematic review by Bugger & Abel points out that the role of MMP-2 a sub group of MMPS, which reduced expression might be of particular interest in understanding the development of cardiac fibrosis. It causes an increased expression of the TGF β and connective tissue growth factor (CTGF) transcription factors are responsible for increased cardiac fibrosis. (Bugger, 2014) Crosslinks increases cardiac stiffness and manifests as early diastolic dysfunction. Furthermore, AGEs can enhance the differentiation of fibroblasts into myofibroblasts which induce ECM dyshomeostasis. Furthermore, as Bugger et. al. proposed it is TGF β, tumour necrosis factor (TNF), angiotensin II and various interleukins which cause fibroblasts and myofibroblasts to respond to disturbed cardiac mechanics. (Souders, 2009) TGF β signalling in myofibroblasts increases the formation of structural ECM proteins and matricellular macromolecules. (Heerebeek, 2007) (Van Linthout, 2008) Another explanation for the formation of cardiac fibrosis than fibroblasts and myofibroblasts are endothelial and epicardial cells which can develop to mesenchymal and myofibroblasts. (Travers, 2016) (Smith C. , 2011) Activated endothelial cells might also be responsible for myocardial stiffness and hence diastolic dysfunction due to the increased uncoupling of endothelial nitric oxide synthase (NOS) to generate superoxide, hydrogen peroxide and peroxynitrite, resulting in diminished nitric oxide (NO) levels. (Franssen, 2016) Reduced NO signaling in endothelial cells and cardiomyocytes increase cardiomyocyte hypertrophy and stiffness as mentioned before.

One other aspect that also contributes to increased fibrotic scarring that even causes contractile dysfunction then arrhythmia, heart failure and often death is disrupted Ca2+ cycling. (Kury, 2018) Intracellular Ca2+ in cardiac cells is maintained through L-type Ca2+ channels for influx respectively natrium calcium exchanger for efflux (Hattori, 2000) but also through Ca2+ release via the ryanodine receptors and uptake by sarcoplasmic reticulum (SR) and mitochondria. (Dhalla, 1978) Changes in SR Ca2+ uptake and release would impair cardiac function. Intra mitochondrial Ca2+ concentration leads to irreversible swelling and mitochondrial dysfunction. This has a severe impact on the energy production of the heart and might contribute to cardiac dysfunction in DbCM. (Duncan, 2011)

11 Mice Models in Cardiovascular Research

Since our understanding of the heart progressed, modern cardiovascular research has become more and more specialized. It is not just studying the heart anymore but research areas focus on specific processes with different functions that are all part of our understanding how the heart works. Amongst them are cardiac metabolism, cardiac function, cardiac structure. To gain this knowledge the contribution of suitable animal models designed to further our understanding between specific cardiac process and a cardiac disease were fundamental. Many findings in rodent models, from basic science, were later confirmed in clinical trials. Today there is a wide variation of animal models in cardiac basic science that the selection of the right model comes down to the specific research question of what should be investigated. (Bugger, et al., 2022)

Mice don't normally develop atherosclerosis. This is important to understand in context with this thesis but also for everybody who is involved with doing mechanistic studies with mice models. The reason for this is that in mice physiology most cholesterol is carried in HDL. (Paigen, 1985) However, as already mentioned atherosclerosis is an important contributor to cardiac dysfunction in humans which is not reflected in the experimental model. So, to make the mice susceptible to atherosclerosis a manipulation of the genes involved in lipoprotein transport is needed. The most commonly used mice models for that are the $Ldlr^{-/-}$ and the $ApoE^{-/-}$ which are described below. To accelerate the development of atherosclerosis, experimental models are fed atherogenic diets that are high in fat and cholesterol which are called Western diets. (Gistera A. , 2022)

11.1 ApoE knockout mice model

It was developed in 1992 and introduced a new era in the research of cardiovascular disease (CVD) making it possible to understanding the pathophysiology of CVD but also evaluate possible therapeutic strategies. It helped to make it possible to understand the complexity of studying a human disease that clinically take a lifetime to result in an apparent event. (Zaragoza, 2011) When accelerated using streptozotocin treatment these lesions can occlude the coronary arteries by the age of 8 months in mouse model. (Tse, 2004) (Gräbner, 2009) Apolipoprotein E (ApoE) is involved in lipoprotein metabolism and lipid transport. It is of vast importance in the production, conversion and clearance of plasma lipoproteins of the blood. ApoE is essential for the ligation of the uptake of remnants chylomicrons and VLDL by the LDL receptor on the surface of hepatic cells to get them out of circulation.
ApoE knockout mice (ApoE-/-) big advantage is that Apo E knockout mice develop atherosclerosis even when fed normal chow. Soon the Apo E knockout model became amongst the most used mouse models to study hypercholesterinemia and the development of atherosclerotic lesions. (Zhang S. , 1992) The biggest disadvantage of the ApoE knockout model is that ApoE has other functions affecting macrophage biology, immune function and adipose tissue biology. All of these could all influence the development of atherosclerosis. Another is, that ApoE which is expressed in bone marrow derived cells such as macrophages or monocytes could contribute to a reduction of atherosclerosis. When transferred ApoE into wild type it can increase the chance of developing atherosclerosis however, this transfer also reduces plasma lipids by which itself contributes to reduction of atherosclerosis. (Getz, 2012) There are many studies

that showed how the ApoE knockout model was used for studying DbCM and how the characteristic morphologic features exhibited by DbCM could be influenced. Toffoli et. al. for instance showed that a TNF-related apoptosis-inducing ligand (TRAIL) could reduce cardiac fibrosis and cardiac apoptosis and thus hinder the development of DbCM. (Toffoli, 2011) Weixin et. al. blocked epidermal growth factor receptor (EGFR) and thus blocked obesity and myocardial inflammation, fibrosis, dysfunction and apoptosis. (Weixin, 2016)

11.2 Ldlr-/- knockout mice model

The $Ldl^{-/-}$ receptor's main function is the endocytosis and removal of circulating LDL cholesterol. It is a glycoprotein which is normally expressed on the hepatocytes. When mutated it leads to the deposition of cholesterol in the vessels helping the development of mild atherosclerosis under normal chow but accelerated atherosclerosis on a high fat diet. (Golfouroush, 2020) It was created in 1993 by Ishibashi et. al. (Ishibashi, Hypercholesterolemia in low density lipoprotein receptor knockout mice and its reversal by adenovirus-mediated gene delivery, 1993) The $Ldlr^{-/-}$ model shares similarities with familial hypercholesteremia in humans a condition with the absence of all functional LDL receptors. (Hobbs, 1990) A reason why $Ldlr^{-/-}$ knockout models are used in medical science is that LDLR do not have these variety of functions as described for ApoE. This reduction of confounders makes results more reliable and easier to interpret as that the atherosclerotic plaque development in $Ldlr^{-/-}$ mice is based solely on plasma lipid levels and no other functions associated with LDL. (Getz, 2012) It has been shown that $Ldlr^{-/-}$ mice develop high plasma cholesterol levels and atherosclerosis. (Zhao, 2020) This can be especially enhanced using a Western diet which can induces more advanced lesions, with a collagen – rich fibrous cap, a core of necrosis and cholesterol clefts and inflammatory cells adjacent to the lumen. (Hartvigsen, 2007) So the $Ldlr^{-/-}$ model became amongst the most used mice model when studying atherosclerosis. It has been shown that the possible formation of an atherosclerotic plaque in three months is three times bigger than in an ApoE knockout model. If a carotid ligation was done the atherosclerotic impact of the lesion was still significantly larger than in an ApoE knockout model. Hence, Torikai et. al. claim that the role of LDL is more important than inflammation and oxidative stress for atherosclerosis research. (Torikai, 2023) Braczko and colleagues found that dyslipidemic $Ldlr^{-/-}$mice develop alterations in cardiac mitochondria which leads to mitochondrial dysfunction. Furthermore, they saw increased oxidative stress, lipotoxicity and apoptosis. (Braczko, 2022) McMillen et. al. saw increased cardiac dysfunction with an altered systolic and diastolic function. (McMillen, 2013) However, if one's research focus is understanding how hypercholesterinemia changes the arterial wall it might still not be ideal as these models are also susceptible to atherosclerotic influences. (Veniant, 2001)

11.3 ob/ob mice model

The development of the ob/ob model came due to a spontaneous mutation at the Jackson Laboratory. This mutation was identified and named leptin in 1994 by Dr. Friedman et. al. Leptin deficiency results in hyperphagia, reduced energy expenditure and extreme obesity. Ob/ob mice normally have elevated HDL plasma cholesterol levels rather than VLDL or LDL. In this sense it is not suitable for studying atherosclerosis as ob/ob mice are actually protected from diet induced atherosclerotic disease.

(Kennedy, 2010) Genetically deficiency in leptin causes an obese and mild non – insulin dependent diabetic phenotype in mice which is normally companied by obesity, glucose intolerance and hyperinsulinemia. (Muzzin, 1996) Obesity is associated with specific alterations in mitochondrial oxidative capacity and the coupling of oxygen consumption and ATP production. The consequence is they can't increase their MV_{O2} and adapt increased workload. They see this as a sign of reduced myocardial efficiency and thus myocardial energetics. Furthermore, there are signs of lipotoxicity. (Boudina, 2005) Intracellular Ca2+ homeostasis and morphological aberrations at the isolated ventricular myocyte level were also seen from Dong and colleagues. They describe major mechanical abnormalities such as depressed peak cell shortening, reduced maximal velocities of shortening and prolonged duration of relengthening in cardiac myocytes. This suggests a cardiac contractile dysfunction which might develop to a LVH. Moreover, they saw signs of cardiac hypertrophy and oxidative stress. (Dong, 2005) In context of DbCM Buchanan et. al. showed that the hearts of ob/ob mice had increased contractility which they believed is due to an increased intravascular volume. Furthermore, they found that the myocardial efficiency is decreased. Both, they see as a stressor for cardiac hypertrophy. (Buchanan, 2005)An advantage of this model is how fast one can see changes in metabolism under a high fat or WD. By the age of two weeks weight changes are visible, by the age of four weeks hyperglycemia with its rise up until three to five months of age. The ob/ob mice also develop hyperlipidemia, temperature regulation abnormalities and are infertile. (Lindstrom, 2007)

11.4 db/db mice model

The db/db mice model is in fact very similar to the ob/ob model with the difference that here mice are resistant to leptin. The db gene encodes a G to a T point mutation of the leptin receptor. The transmission is done autosomal recessive. The leptin receptor mutation ($LepR^{db/db}$) results in abnormal splicing and a defective receptor for leptin. (Tesch, 2011) This leads to an overexpression of circulating leptin and a complete deficiency of the long isoform of the leptin receptor (ObRb). Except that the phenotype is very similar regarding hyperphagia, hypometabolism, and obesity but different in glucose metabolism. In this aspect they are very similar to humans in their phenotype and co – morbidities. (Sullivan, 2015) Db/db mice develop higher glucose levels and hence can be used to study diabetes and associated disease. The reason for different blood glucose levels is not yet completely understood but is assumed in the different gut microbiota composition. (Yang, 2019) (Suriano, 2021) db/db mice are interesting to research because they have a relative short life span. Hyperinsulinemia can be apparent by two weeks life, hyperglycemia and hyperinsulinemia by the time of 4 weeks. Hence, they are ideal for short time rodent studies. (Srinivasan, 2007) Hafstad and colleagues found a deranged cardiac metabolism with increased signs of lipotoxicity, increased oxidative stress in the hearts of db/db mice. (Hafstad, 2006) This was confirmed by How et. al. who further found an impaired cardiac efficiency with an impaired SV_{O2}. Furthermore, they saw an impaired ventricular function with impaired values for end-diastolic, as well as the end-systolic, pressure-volume relationships. They see this as sign for concentric hypertrophy and reduced compliance. Furthermore, they see signs of diastolic dysfunction, an impaired calcium reuptake in the sarcoplasmic reticulum and hence impaired relaxation. (How, 2006) Contractile dysfunction can also be seen as Aasum and colleagues found. In

their experiments db/db mice showed systolic and diastolic dysfunction. (Aasum, Age-dependent changes in metabolism, contractile function, and ischemic sensitivity in hearts from db/db mice, 2003)

11.5 SRBI knockout mice model

Scavenger receptor class B, type I (SRBI) is an HDL receptor that regulates the selective uptake of plasma HDL cholesterol by the liver. It can be found on the surface of numerous cell types. The SRBI model is often used to study myocardial infarctions as it faster leads to significant coronary artery lesions. HDL inversely correlates with the development of atherosclerosis to its role in reverse cholesterol transport. Under physiological conditions the reverse cholesterol transport should help the organism to regulate elevated HDL levels. HDL is important in the progression of atherosclerosis but also plays a role in inflammation. (Golfouroush, 2020) In the SRBI model this is not possible, promoting atherosclerosis. Knock out mice models with a homozygous SRBI deficiency have a twofold higher increase in plasma cholesterol. This consists primarily out of un- esterified and esterified cholesterols within larger and heterogenous HDL particles. (Rigotti, 1997) Targeting SRBI also leads to an increase of biliary cholesterol which cannot be transported back to the liver or removed by the gall bladder. Many studies in murine models proved that SRBI has a major role in the development of atherosclerosis. Knocking it out can actually promote its development while inducing it can have an antiatherogenic effect. (Kozarsky, 2000) (Takeshi, 1999) Many hypothesis for treating atherosclerosis and associated cardiovascular disease base on SRBI and all relevant factors implicated in its regulation and their potential application as a drug target. (Leiva, 2011)

11.6 PCSK9 (D374Y) mice model

If present in the circulation, the recently discovered PCSK9 can bind LDL receptors and mark them for lysosomal degradation. PCSK9 (D374Y) is a gain of function mutation which is induced to the mice by a single venous injection of an adeno - associated virus. By that it disrupts the endocytic recycling of $Ldl^{-/-}$ receptors and leads to elevated cholesterol levels under a normal chow but a severe hypercholesterinemia under a western diet in mice. (Gistera, 2022) In 2005 Rashid et. al. confirmed that a PCSK9 inactivation is associated with threefold higher LDL levels in the liver and a drastic LDL reduction in plasma. (Rashid, 2005) Mice lacking PCSK9 have 40% to 50% lower circulating cholesterol levels, approximately 80 % less LDL in plasma and three to fourfold higher levels of total liver LDLR protein. (Zaid, 2008) The first study of PCSK9 and it enhancement of atherosclerosis was done by Herbert et. al. which showed that after a 15 - weeks long trial PCSK9 knockout mice exhibited extensive atherosclerotic plaques compared to wild type. (Herbert, 2010) This was supported by a single injection of recombinant adeno-associated viral vectors encoding PCSK9-D374Y which induced atherosclerosis in mice (Bjorklund, 2014) These studies suggest that PCSK9 support the development of atherosclerosis and exacerbate inflammation. So, to demonstrate the relationship between PCSK9 and atherosclerosis research was done overexpressing or silencing the PCSK9. It showed that overexpression is proatherogenic and its absence is protective. (Denis, 2012) (Tang Z. , 2017) (Seidah, 2022)

11.7 Lipoprotein (a) transgenic mice model

Lipoprotein (a) is a LDL particle that is associated with proinflammatory and proatherogenic properties. Its plasma levels and a high lipoprotein are well established risk factors for coronary artery disease in humans. High lipoprotein (a) levels are due to a high production of lipoprotein (a). This is a huge advantage of this model: to simplify the experimental situation: a high level of lipoprotein equals a high risk for cardiovascular disease. This situation is completely similar as in humans. However, different to humans there is circulating nonlipoprotein (a) in mice models which can influence the model. (Gistera, 2022) The most useful application of the Lipoprotein (a) transgenic mouse model is the assessment of the role of lipoprotein a in the progression of the development of atherosclerosis. In vitro experiments have shown great promise but there is no evidence that it is the same in humans. (Marcinova, 2002) Evidence to prove that apo(a) is atherogenic first came from Lawn. et. al. who found that apo(a) transgenic mice had significantly higher aortic lesions. (Lawn, 1992) This finding very soon became center of a heated debate. There were studies which supported it like Callow et. al. (Callow, 1995) but then were those who contradicted it like Mancini et. al. (Mancini, 1995) However, Berg et. al. showed that throughout a lifetime on normal food lipoprotein (a) transgenic mice had a greater extent of atherosclerotic lesions. (Berg, 2002) Thus, it became consent, to see lipoprotein a as a risk factor for cardiovascular disease.

11.8 High Fat Diet

In rodent models high – fat diets (HFDs) consists of chow which have 45% to 60% of the total energy (kcal) of fat sources and stem mostly from saturated fatty acids (FA). A feeding period of 8 to 12 weeks has shown increased body weight, blood glucose, FA, cholesterol, triglyceride (TG) and insulin levels in the mouse model. (Ge, 2010) In experimental studies this diet caused minimal left ventricular hypertrophy and remodeling and impaired cardiac function minimally. Enhanced FA oxidation and reduced glucose oxidation has shown no effect on the cardiac energy status as mitochondrial function was unaffected. The development of insulin resistance through this diet has shown possible but takes several weeks. (Zhang L. , 2010) The presence of increased cardiac triglycerides but also reactive long-chain acyl-CoAs, ceramide, cholesterol, diacylglycerol, and acylcarnitines promotes the hypothesis of cardiac lipotoxicity. If the duration of the HFD is longer than 20 weeks it appears that myocardial levels of OXPHOS proteins may also decrease without impairing energy functions due to impaired respiratory functions. (Brahma, 2020) The presence of left ventricular dysfunctions such as cardiac hypertrophy and consequently dysfunction appears to be conflicting as it only has been reported about it in some studies. (Tadinada, 2021) (Wang Q. , 2016) Oxidative stress, apoptosis, fibrosis, and impaired Ca^{2+} handling may be responsible for impaired structural and metabolic cardiac dysfunction observed in these models but the foundation of the mechanisms behind it has not been understood yet. (Bugger H. , 2022)

11.9 High Sugar Diets

A high sugar diet used in cardiovascular research consists of high sucrose or high fructose needs a continuing feeding period of more than four months to induce cardiac hypertrophy, dysfunction, and impaired contractile reserve. (Wright, 2009) High Sugar Diets are characterized by an early reduction of cardiac glycolysis and glucose oxidation

rates, increased FAO rates. Furthermore, they have a decreased cardiac metabolic response to insulin, which causes myocardial energy deprivation due to impaired ATP regeneration. From this point of view, they are very similar to the metabolic changes seen in fundamental obesity or T2DM. (Luptak, 2019) Myocardial energy deprivation might be associated with impaired function of energy metabolic proteins in FA utilization, glycolysis, TCA cycle, or OXPHOS. (Bugger H. , 2022)

11.10 Streptozotocin

Streptozotocin (STZ) is a β-cell toxin which leads to insulin – deficient diabetes, hyperglycemia and hyperlipidemia. STZ leads to hypotrophy of the cardiomyocytes which is alleged to be due to increased protein degradation as a result of insulinopenia. The cardiac contractility is also decreased. (Hall, 1996) Under STZ treatment hearts typically show reduced glucose uptake, increased fatty acid uptake and fatty acid oxidation. However, the incorporation of fatty acids into cardiac phospholipids and triglycerids seemed increased. (Hasselbaink, 2003) (Bugger H. , 2012) Increased fatty acid utilization results in an increae in myocardial O2 consumption which shows reduced cardiac efficiency. (Aasum, 2006) Streptozotocin treatment can be used together with high fat diets to express high levels of T2DM and incorporate more aspects of human T2DM which are not replicated in common rodent models. (Bugger, et al., 2022)

12 Rationale

Obesity and Type 2 diabetes mellitus (T2DM) are well established risk factors for cardiovascular diseases including diastolic dysfunction. Animal models of obesity and T2DM are commonly used to investigate mechanistic features of cardiovascular disease such as diastolic dysfunction but fall short to include the development of atherosclerosis. This is because physiologically mice cannot develop atherosclerosis similar to humans. However, in human cardiovascular disease atherosclerosis progressions is a big driving factor for the cardiac dysfunction. Thus, the aim of this current study was to investigate the effects of obesity and T2DM on cardiac function and structure in a mouse model that also develops atherosclerosis.

13 Materials & Methods

13.1 Animals

Ldlr$^{-/-}$ male mice (C57BL/6J) were purchased by Jackson Laboratories (Bar Harbor, Maine, USA).

All protocols involving rodents were approved by the ethics committee of the Austrian Ministry of Science and conform to the high ethical standards of the Medical University Graz. All experimental procedures were carried out in accordance with the Declaration of Helsinki.

13.2 Food

For the Western diet group, food was consisting of a high-fat and high-cholesterol diet consisting of 42kJ% of fat, 15kJ% of protein, and 43 kJ% of carbohydrate which was

provided by ssniff Spezialdiäten GmbH (Soest, Germany). This high-fat and high-cholesterol diet corresponds to an energetic equivalent of 19.1 MJ/kg or 4,575 kcal/gk.

13.3 Study

In this study the effect of a Western diet (WD; high-fat and high-cholesterol diet) on the cardiac function of Ldlr$^{-/-}$ mice was studied. Ldlr$^{-/-}$ male mice (C57BL/6J background; Chow group n=10, WD n=10) were purchased by Jackson Laboratories (Bar Harbor, Maine, USA) and arrived at the laboratory of experimental cardiology of the Medical University of Graz at the age of 6 weeks where they had one week to accommodate, before being placed on standard chow diet or WD for the duration of 16 weeks.

All mice were group housed (2-3 mice per cage) in ventilated cages at 22^{0}C in a pathogen-free animal housing facility. Day and night cycles were simulated by 12-hour periods of light. The study began following 1 week of acclimatization. Mice had access to food and water ad libitum. Body weights, food, and water intake were measured every week. At 8 weeks, in vivo experiments were done for the first time, to establish an experimental phenotype. These were glucose tolerance tests, and echocardiography.

At 16 weeks, just before the harvest all in vivo experiments were repeated to investigate the progression of a high fat diet on the phenotype.

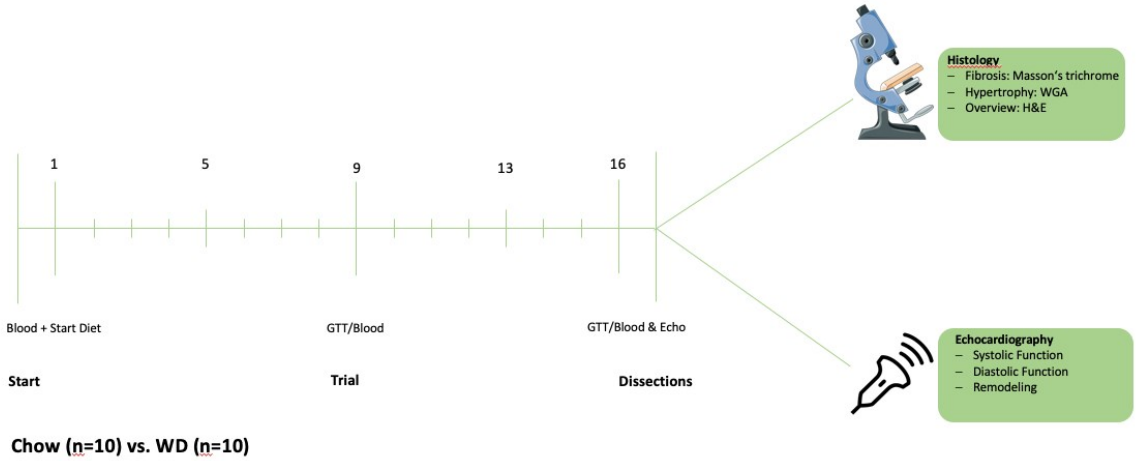

Figure 3: Project Plan

Sacrifice was done per neck dissection after an isoflurane inhalation and making sure that each animal was deeply sedated. All experiments were carried out according to the high ethical standards of the Medical University Graz. The study was also presented and approved by the ethics committee of the Austrian Board of the Ministry of Sciences. All experimental procedures were carried out in accordance with the Declaration of Helsinki.

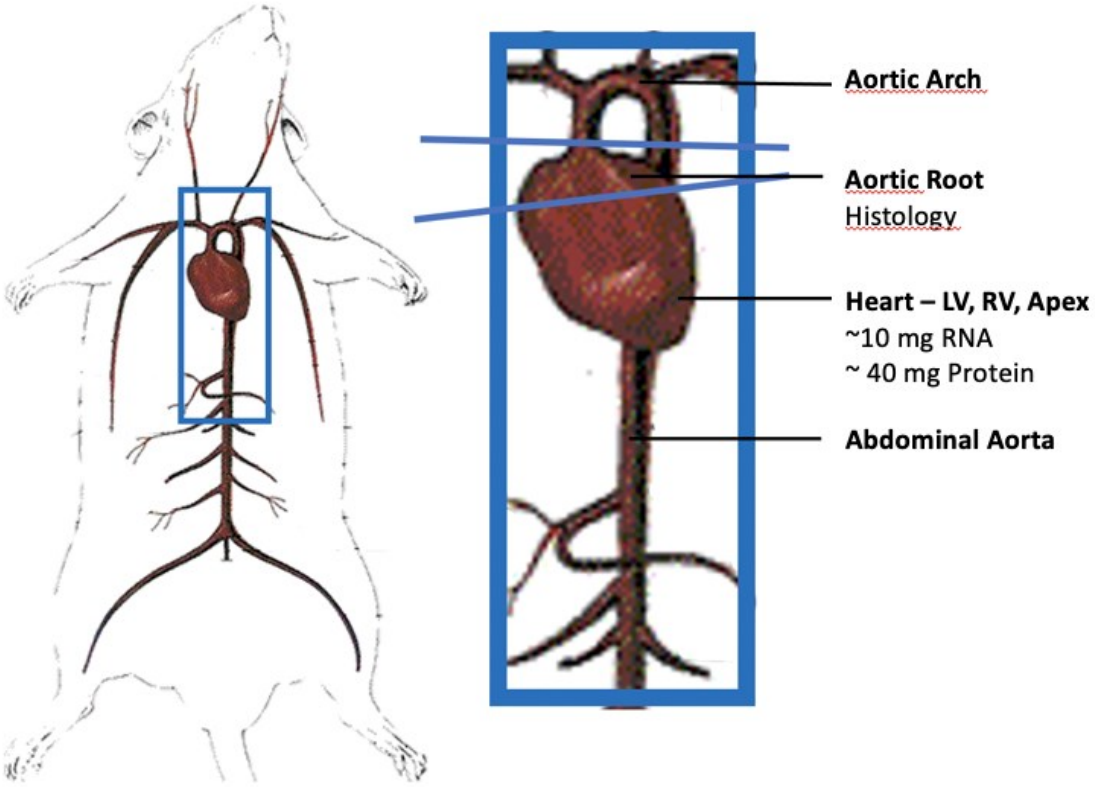

Figure 4: Tissue distribution of the heart

At the harvest, the heart was removed, weighed and cut into 3 sections: aortic arch, aortic root, and heart as depicted by the blue lines in (Figure 4). The aortic root was embedded in OCT to be used in experiments for histology. The left ventricle, right ventricle, and apex were cut and weighed again to be used for protein work and molecular work at a later stage.

Other than the heart, the liver, kidney, spleen, and white adipose tissue, were harvested and kept for later use. The tibia length of the right tibia was measured with a caliper. All tissues were shock frozen in liquid nitrogen and stored in a -80^{0}C freezer.

13.4 Consumables

Table 3: Consumables

Glucose Test Strips	Accu-Check Performa, Indianapolis USA
Injection needles	B Braun; Meisungen, Germany
Injection syringes	B Braun; Meisungen, Germany
Leica Cryofect (LCR4 P301212)	Leica Biosystems; Mannheim, Germany
Object Carriers	Carl Roth GmBh; Karlsruhe, Germany
Scigen Tissue Plus OCT Compound (#4586)	Fisher Scientific; Waltham, Massachusetts, USA
PAP pen	Sigma Aldrich, Darmstadt, Germany
Pipette tips	Eppendorf, Hamburg, Deutschland
Pipettes	Eppendorf, Hamburg, Deutschland
Reaction tubes	Eppendorf, Hamburg, Deutschland

Thermo Scientific Superfrost plus microscope slides (J1800 AMNZ)	Fisher Scientific, Waltham, Massachusetts, USA

13.5 Chemicals and Reagents

Table 4: Chemicals and Reagents

4% Paraformaldehyd	Morphisto; Frankfurt, Deutschland
Acetic Solution (#3738.1)	Carl Roth GmBh; Karlsruhe, Germany
Aniline Blue Solution (#HT 154-250ML)	Sigma Aldrich, Darmstadt, Germany
Bouin's solution (#HT10132-1L)	Sigma Aldrich; Darmstadt Germany
Biebrich Scarlet Acid Fuchsin (#HT151-250ML)	Sigma Aldrich, Darmstadt, Germany
Dako Fluorescence Mounting Medium	Dako; Carpinteria, California, USA
Ethanol (#K52570083 026)	Sigma Aldrich; Darmstadt, Germany
Isoflurane	Piramal Critical Care; Schelden Circle, Bethlehem, USA
Phosphotungstic Acid Solution (#HT152-250ML)	Sigma Aldrich; Darmstadt, Germany
Phosphor molybdic acid (#HT153-250ML)	Sigma Aldrich; Darmstadt, Germany
Roticlear	Carl Roth GmBh; Karlsruhe, Germany
Rotimount (#HP68.1)	Carl Roth GmBh; Karlsruhe, Germany
Weigert's iron hematoxylin Part A (#HT107-500ML)	Sigma Aldrich; Darmstadt, Germany
Weigert's iron hematoxylin Part B (#HT109-500ML)	Sigma Aldrich; Darmstadt, Germany

13.6 Programs and Machines

Table 5: Programs & Machines

Blood Glucose Meter	Accu-Check Performa, Indianapolis USA
Centrifuge 4C^0 Heraus Fresco 21	Thermo, Electron LED GmbH, Osterode, Deutschland
Cryotome HM 560	ThermoFisher, Walldorf, Germany
Fluroscence Microscope BX 51	Olympus, Vienna, Austria
Graph Pad Prism 9	GraphPad Software Inc, San Diego, California, USA
Olympus CellSense Standard	Olympus Life Science, Waltham, Massachusetts, USA
Spectrophotometer Spetra Max 384	Molecular Devices Corporation, San Jose California, USA
Vevo 3100, Vevo imaging Systems	FUJIFILM VisualSonics Inc. Toronto, Canada

Vevo Lab analysis software	FUJIFILM VisualSonics Inc. Toronto, Canada
Vortexer	IKA, Stauffe, Germany

13.7 Experiments

All methods of the experiments used in this study were established and refined by the research group for experimental cardiology "Cardiac Energetics" led by principal investigator Assoz. Prof. Priv.-Doz. Dr. Heiko Bugger.

13.8 Bodyweight, Physiological ratios, Food & Water Intake

Food and Water consumptions were monitored every week. Assuming an equal consumption, the mean per cage was then calculated. Bodyweight was monitored every week too. After sacrifice physiological ratios commonly used in metabolic research like the heart–tibia length ratio and heart–body weight ratio were calculated.

13.9 Glucose Tolerance Test

The mice were fasted 4-5 hours. The tip of the tail was cut with a scalpel blade and the first drop of blood was discarded. The blood glucose was measured with a blood glucose meter Body weight and blood glucose were determined at T=0 minutes. Mice then received an intraabdominal (i.p.) injection of 40% sterile glucose diluted 1:4 in 0,9% NaCl to reach a dose of 2g/kg. After injections, the blood glucose was taken at 10, 20, 30, 60, 90 and 120 minutes.

13.10 Transthoracic Echocardiography

Transthoracic echocardiography was done on Vevo 3100 by Vevo® imaging systems. Beforehand all mice received the anesthetic isoflurane by inhalation. While doing transthoracic echocardiography calm handling of the mice was important as heart rates had to be between 400-500 beats per minutes for the echocardiography scan to be usable. At the beginning, mice were placed on the back with their arms and legs fixed on the echocardiography platform, to expose the sternum. Furthermore, a temperature probe was applied rectally.

To accomplish the best scan of the parasternal long-axis view (PSLAX) the echocardiography platform was tilted up, so the animal's head and the left side are highest is to shift the heart down in the chest. When scanning, the transducer was angled parallel to the sternum and then rotated approximately 15-35^0 counterclockwise to face toward the right shoulder of the animal.

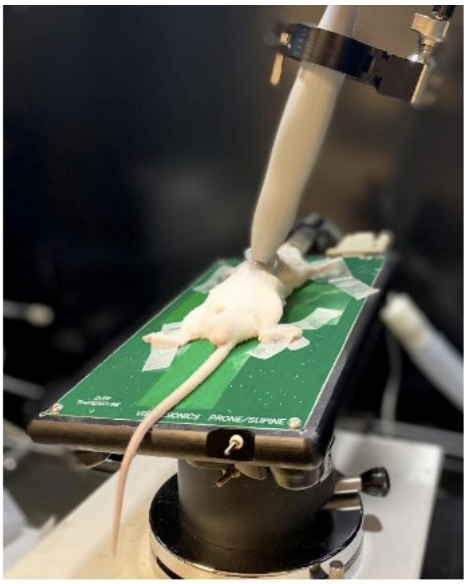

Figure 5: PSLAX animal position

Image from (FUJIFILM VisualSonics, Inc., n.d.)

A quality sign for a good view in B - mode is the sternum and the aorta in a horizontal line. From the B – mode view, a left ventricular trace in M – mode for measuring systolic function can be recorded.

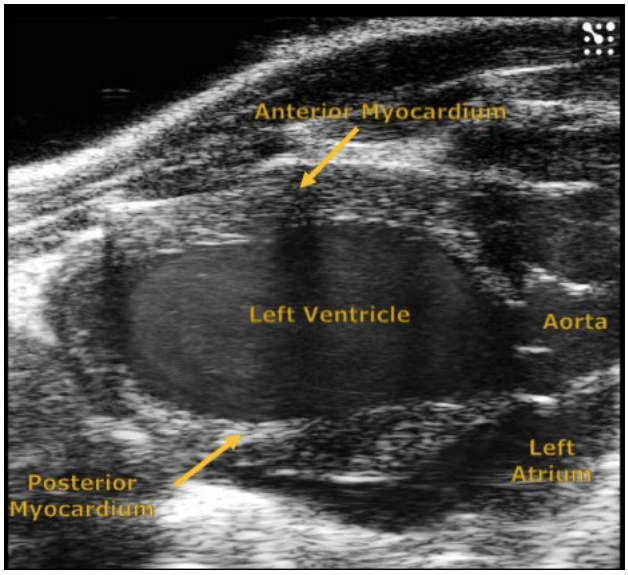

Figure 6: PSLAX view

Image from (FUJIFILM VisualSonics, Inc., n.d.)

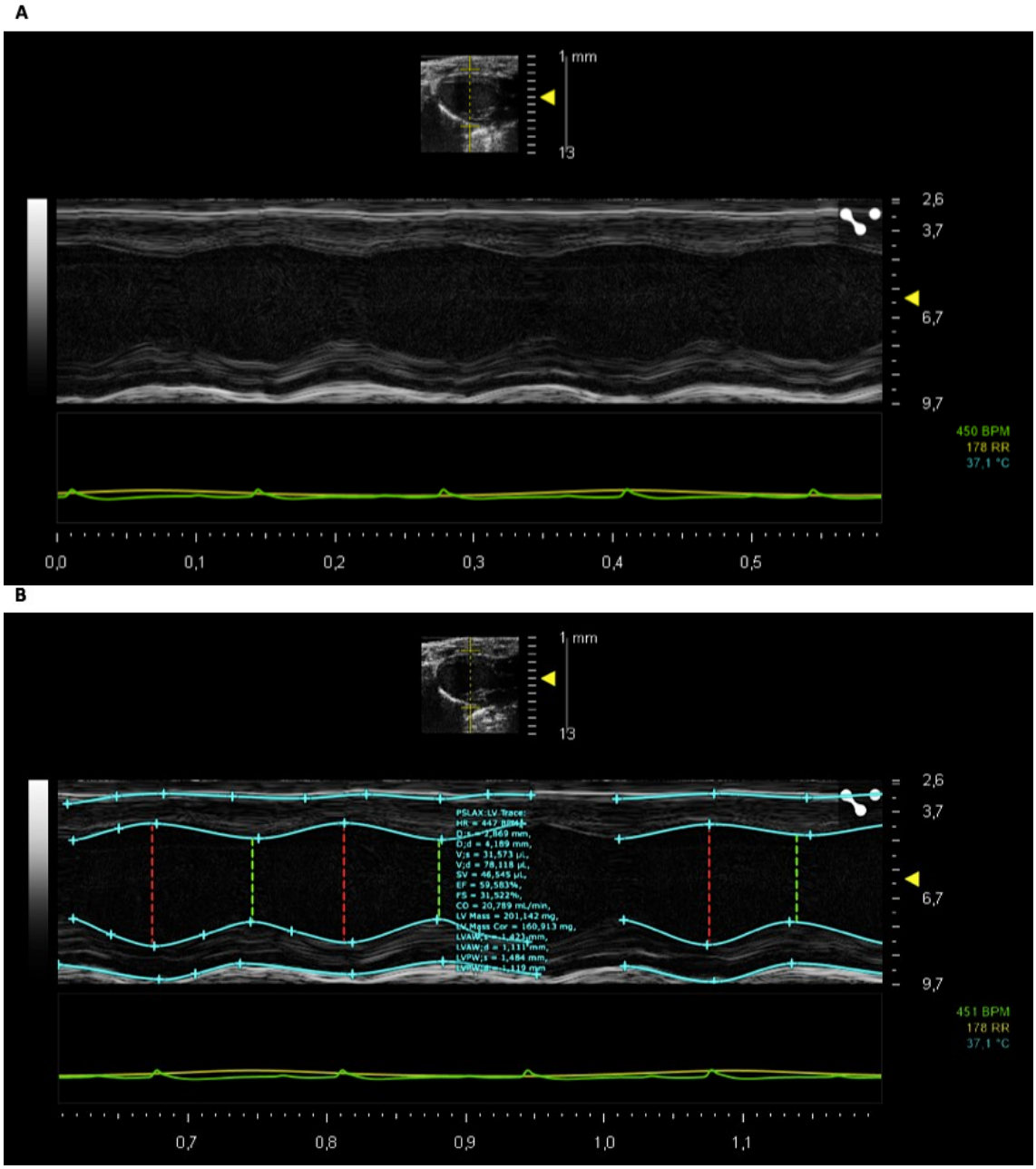

Figure 7: (A) PSLAX loop (B) LV – trace

Systolic Function was interpreted by adding a left ventricular trace in the PSLAX. This was done in the Vevo lab analysis software. For the lv-trace, it is important to identify the left ventricular anterior and the left ventricular posterior wall in the echo correctly. All measurements were repeated at least 6 times to ensure a representable mean.

Parameter	Units
Depth	mm
Heart Rate	BPM
Diameter;s	mm
Diameter;d	mm
Volume;s	uL
Volume;d	uL
Stroke Volume	uL
Ejection Fraction	%
Fractional Shortening	%
Cardiac Output	mL/min
LV Mass	mg
LV Mass Cor	mg
LVAW;s	mm
LVAW;d	mm
LVPW;s	mm
LVPW;d	mm

Table 6: Left ventricular trace

The left ventricular trace gives all the following measurements, as seen above, of a representative example in (Table 6).

After the PSLAX view the short axis view (SAX) can be recorded. For that the transducer was rotated 90^0 clockwise from the PSLAX in B - mode. A quality sign for a good SAX has the papillary muscles at 2 and 4 o'clock shown.

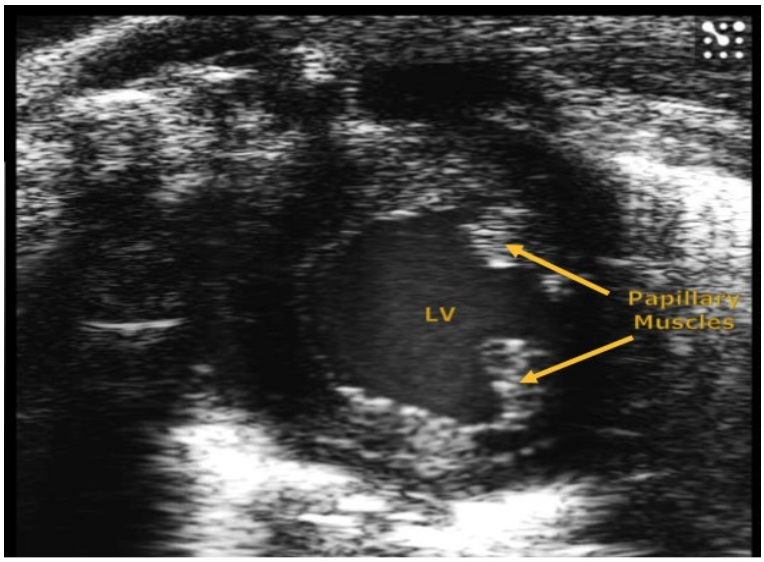

Figure 8: SAX view

Image from (FUJIFILM VisualSonics, Inc., n.d.)

From the SAX view the apical four-chamber view was obtained by adjusting the transducer steeper, at least 45^0 towards the mouse's right shoulder. Furthermore, the probe was adjusted slightly below the rib cage towards the apex of the heart.

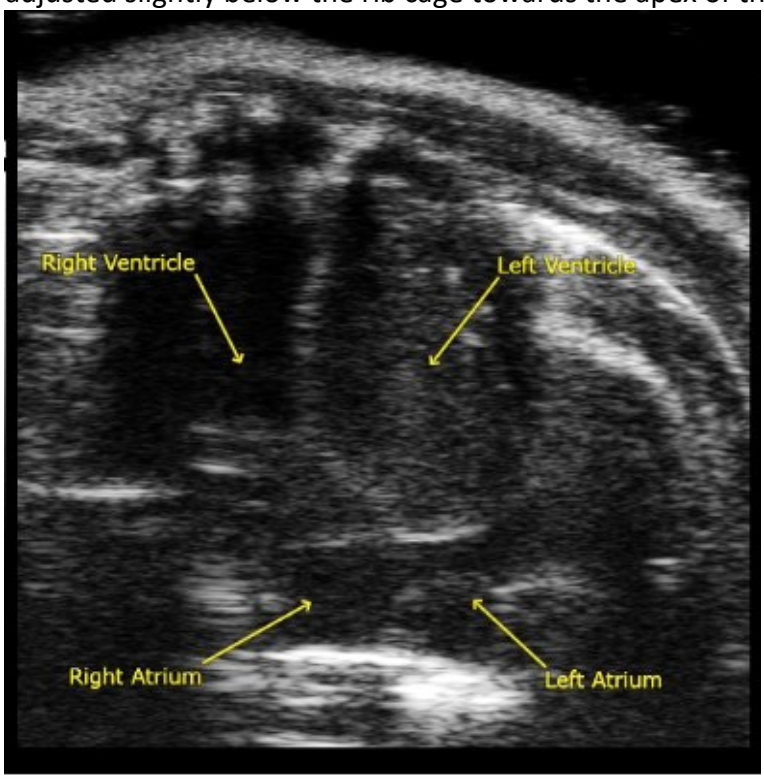

Figure 9: Apical four-chamber view

Image from: (FUJIFILM VisualSonics, Inc., n.d.)

The apical four-chamber view is important to identify the mitral valve. At the annulus of the mitral valve, the mitral valve flow can be recorded using the pulsed wave Doppler mode.

A

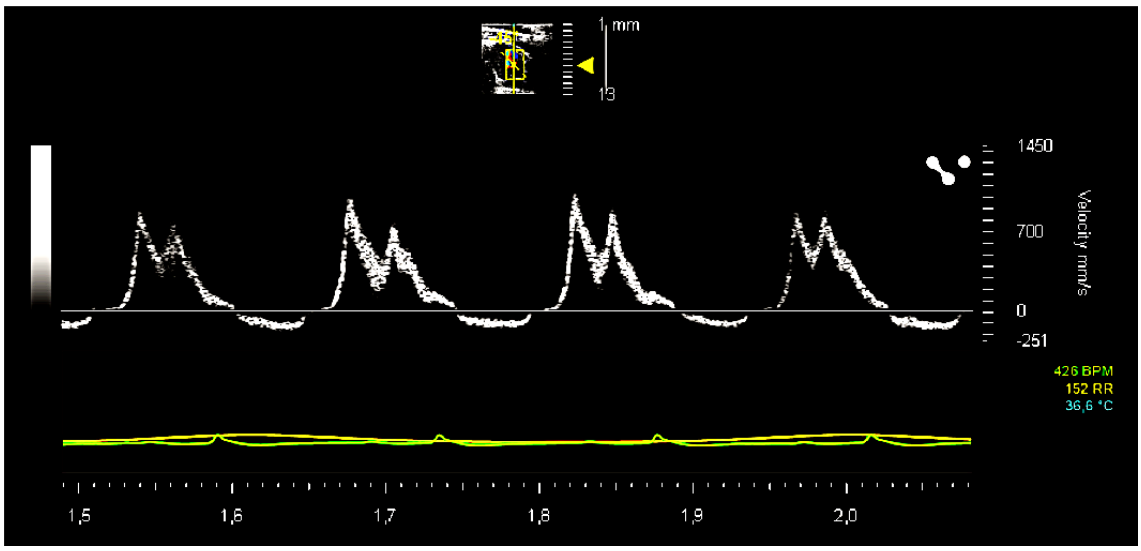

B

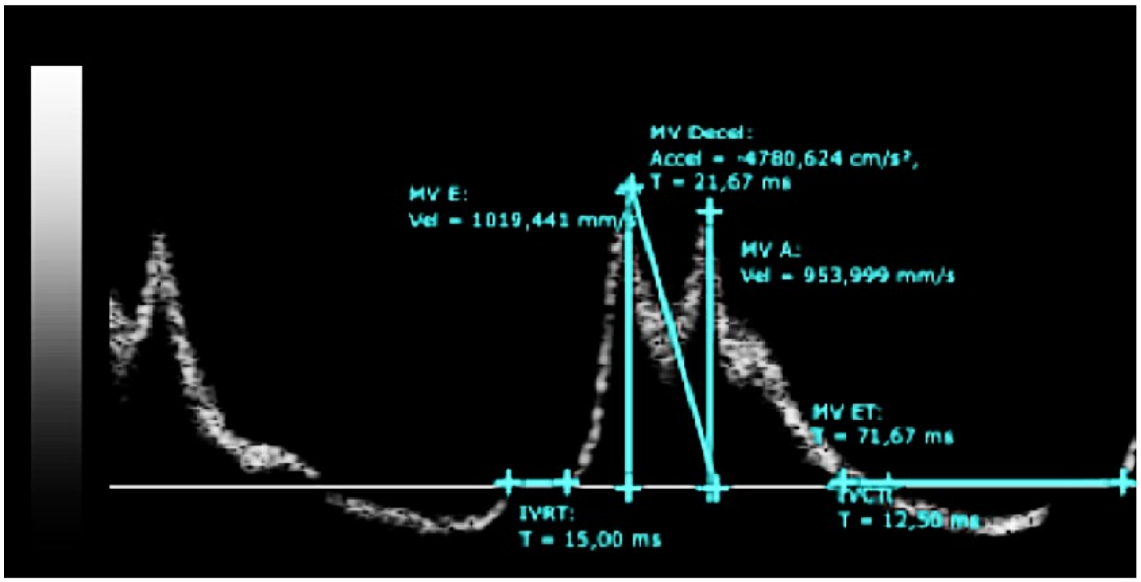

Figure 10: Pulsed wave Doppler:

(A) Pulsed wave Doppler without measurements , **(B)** Pulsed wave Doppler with measurements

In the Pulsed wave Doppler (Figure 10B**)**, the movement of the mitral septal wall is recorded. Analyzing Pulsed waved Doppler, one gets the E wave, A wave, the mitral valve deceleration time, MV deceleration time, the interventricular relaxation time, IVRT, the interventricular contraction time, IVCT, and the mitral valvular ejection time, MV ET.

Next, in pulsed wave tissue Doppler mode the movement of the mitral septal wall can be recorded. Both the recordings of the mitral valve flow of pulsed wave Doppler and the tissue motion of pulsed wave tissue Doppler are necessary to calculate the diastolic function. (FUJIFILM VisualSonics, Inc., n.d.)

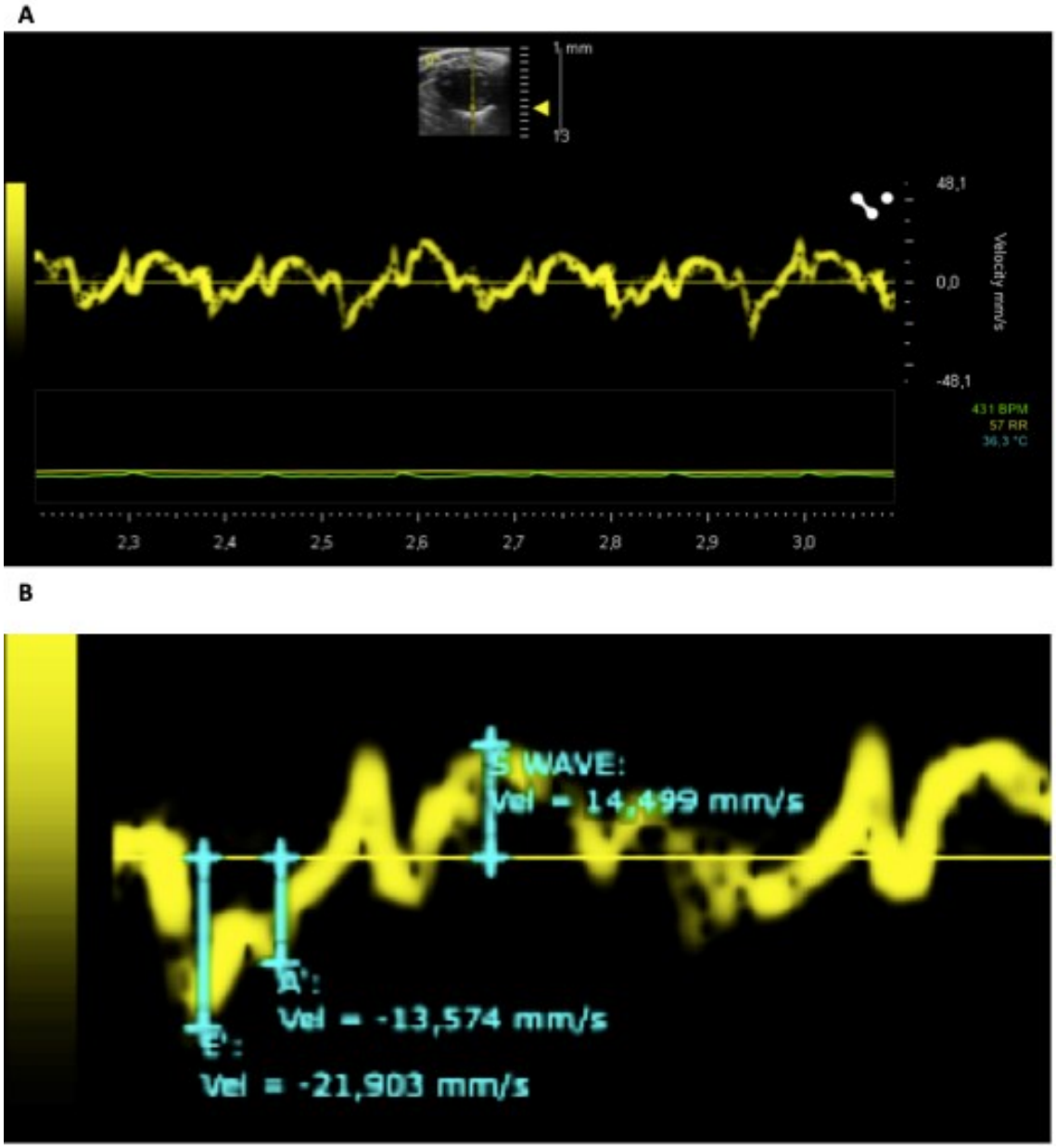

Figure 11: Pulsed wave tissue Doppler

(A) Pulsed wave tissue Doppler without measurements, **(B)** Pulsed wave tissue Doppler with measurements

In Tissue Doppler (Figure 11B) the velocity for early diastole, E', late diastole during atrial contraction (A'), and the peak systolic annular velocity (s') were measured. Again, each measurement was repeated six times to ensure a good reliable mean.

MV E/E' is the most common parameter for measuring diastolic function in echocardiography. It is actually composed of two views: Pulsed wave Doppler and Pulsed wave tissue Doppler. E–wave represents the pressure gradient between the left ventricular atrium and left ventricular ventricle as well as the left ventricular compliance. E' represents the velocity of the left ventricular relaxation. All these parameters are measured at the mitral valve. They can be impaired in cardiac diastolic dysfunction. Since it is composed of two different views MV E/E' is more reliable than the other established parameter for assessing diastolic function MV E/A. It represents the blood flow from left ventricular

relaxation, E wave, in early diastole to peak velocity flow in late diastole, A wave. However, its interpretation is often problematic as it is more susceptible to disturbance factors such as heart rate and heart rhythms.

All echocardiography recordings were analyzed using the software Vevo Imaging Systems. Recordings analyzed were left ventricular traces in the PSLAX, pulsed wave Doppler, and pulsed wave tissue Doppler recordings. All echos in this study were done by Nikole Byrne Ph.D. and analyzed by myself.

13.11 Histology

13.11.1 Cryotome

Histology slides were prepared on the Thermo Scientific Cryostat Microm Cryo Star HM 560. The cryotome had to be disinfected 30 minutes before use with Leica Cryofect and its settings had to be set to a blade temperature of -20°C, an object temperature -17°C. Thin sectioning was set at 4µm, thick sectioning at 30µm. Then the cryotome was left to cool down to reach the temperature which was set previously.

After 30 minutes an OCT sample was put in the cryotome chuck using OCT to hold. Before a blade was inserted in the blade holder. During cutting, all samples were first trimmed with the 30µm sectioning to get to the right spot. The right spot for this thesis was when both chambers of the heart showed fully for the first time. As soon as this was visible, a series of 10 slides with three cuts per slide was picked up using a brush.

Slides were then left overnight in a -20 °C freezer, before being stored, for long time storage, in a -80 °C freezer.

13.11.2 H&E Stain

Hematoxylin and Eosin stains was used as an overview image. Slides were circled using a PAP pen. Then slides were incubated in 4% PFA for 5 minutes, followed by rinsing for 1 minute in warm running water. Slides were then place in hematoxylin for 5 minutes, rinsed for 10 minutes, then stained by eosin for 10 minutes, then washed 3 times for 1 minute again in 3 different staining trays filled with ddH_2O. Finally, all slides were drained using a dilution series of ethanol (EtOH): 1 min in 70%, 30 seconds in 90%, and 30 seconds in 100% EtOH. Before they were covered using Roti®-Mount and a cover slip all slides were cleared in Roticlear®. All slides were pressed for 10 minutes and dried overnight, then stored in a box at room temperature.

13.11.3 WGA Stain

Cardiac Hypertrophy can be quantified using the histological stain WGA. It stains the cardiomyocytes. Its size can then be measured and analyzed.

For WGA staining, after all slides had thawed, all cuts were circled using a PAP pen. After that they were fixated in PFA 4% for 15 minutes and washed 3 times for 3 minutes in PBS Approximately 800 µl WGA solution was pipetted on the cuts and left to incubate for 1 hour in the dark. WGA solution consists of 1mg/ml of WGA stock at a 1:100 concentration diluted

with PBS. After the incubation, the washing step of 3 minutes in 3 staining trays of PBS was repeated using fresh PBS.

In the end, all slides were embedded with a drop of Dako Fluorescence Mounting Medium and covered with a coverslip. They were left to dry in a fluorescence nonpermeable box in the freezer overnight, before they could be imaged on a fluorescence microscope.

For the analysis of the cardiomyocyte size, 4 randomly chosen areas per cut at an enlargement of 40 times were imaged. This was done using the software Olympus CellSense Standard. In these images, 30 cardiomyocytes were circled. The corresponding size was then given in µm by the software. For the WGA quantification, 3 cuts with 4 areas and 30 cardiomyocytes per area were analyzed equaling 3600 cardiomyocytes that were measured and compared in size.

13.11.4 Masson's Trichrome Stain

Masson's trichrome stain is one of the most common histological stains to show cardiac fibrosis.

The preparation for Masson's Trichrome stain took two days. On the first day, all slides were thawed, dried, and circled using a PAP pen. After fixation for 1 hour in PFA 4% they were incubated in Bouin's solution overnight at room temperature.

The next day all slides were washed in warm water for 2 minutes and rinsed shortly in ddH_2O to wash off Bouin's solution. They were then stained in Weigert's iron hematoxylin working solution and left to incubate for 5 minutes at room temperature. Weigert's iron hematoxylin working solution was washed off 3 times for 3 minutes in different staining trays filled with ddH2O. Next, phosphotungstic acid solution/phosphor molybdic acid was pipetted on all slides 3-4 times in 10 minutes. Here it was important to constantly keep all cuts covered and wet. Without washing, all slides were stained in aniline blue solution for 5 minutes before being washed 3 times for 3 minutes in ddH_2O. Before all slides were drained in an ethanol dilution series at 70%, 90% & 100% ethanol for 3 minutes each, they were incubated in 1% acetic acid and washed with ddH2O for 2 times 1 minute each. Finally, all slides were cleared in Roticlear® for 5 minutes and embedded with Roti®-Mount and a cover slip. After pressing for 10 minutes they were let dry overnight. Slides were could then be kept in a box at room temperature.

For analysis 4 randomly selected spots per cut were imaged at a 20 times enlargement using a light microscope. These images were then quantified for fibrosis using the software ImageJ.

13.12 Analysis & Statistics

Statistical analysis and graphs used in this thesis were done using Graph Pad Prism 9. All statistics involving the comparison of two groups were done using unpaired t-tests. As standard error, the standard error of the mean (SEM) was used. Significance levels were accepted as $p < 0.05$ and marked as * respectively for $p < 0.01$ as ** and for $p < 0.001$ as ***. Values far away from the data collected were checked for plausibility, and then if not plausible excluded from analysis on the basis being measurement errors.

14 Results

14.1 Physiological Data

Table 7 Bodyweight of Chow and WD - fed Ldlr$^{-/-}$ mice during 16 weeks of diet

Time (wks)	1	2	3	4	5	6	7	8	9	10	11	12	13	14	15	16
Chow	25,30 ± 0.68	25,78 ± 0.64	26,58 ± 0.68	26,86 ± 0.78	27,69 ± 0.75	28,05 ± 0.71	28,83 ± 0.65	27,54 ± 0.53	28,75 ± 0.68	29,26 ± 0.66	28,99 ± 0.63	29,43 ± 0.67	29,50 ± 0.68	29,88 ± 0.69	29,49 ± 0.63	30,25 ± 0.77
WD	25,06 ± 0.81	26,28 ± 0.70	27,50 ± 0.69	28,48 ± 0.78	29,76 ± 1.02	30,91 ± 1.01	32,02 ± 1.16	31,72 ± 1.13	32,33 ± 0.96	33,05 ± 1.15	34,03 ± 1.25	34,97 ± 1.11	35,84 ± 1.27	36,58 ± 1.39	37,04 ± 1.64	37,19 ± 1.20
Chow/WD	ns	*	***	***	***	***	***	***	***	***	***	***	***	***	***	***

Chow n = 11, WD n = 10, unpaired t – test, mean ± SEM; *p <0.05, **p<0.01, ***p<0.001

Table 7 shows weekly measurements of body weight in response to 16 weeks of Chow or WD feeding. Body weight increased steadily over the 16 weeks of study in both groups. 2 weeks after initiation of the feeding protocol and at any timepoint thereafter, body weight was increased in the WD group compared to the chow group.

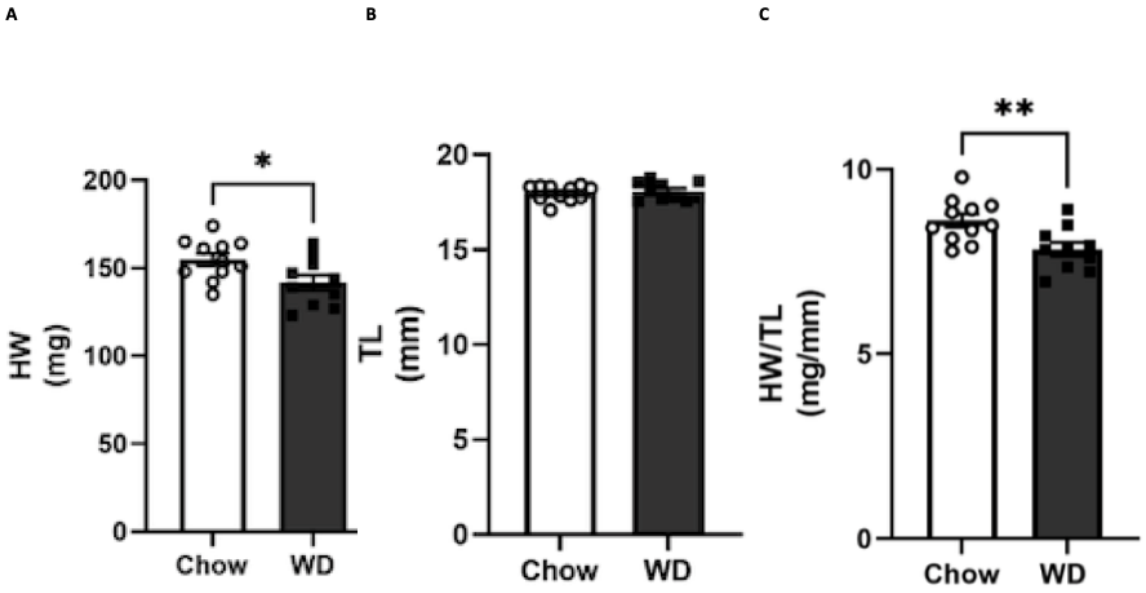

Figure 12: (A) Heart Weight (B) Tibia Length (C) Heart Weight/Tibia Length ratio of Chow and WD - fed Ldlr$^{-/-}$ mice during 16 weeks of diet

(A) Heart Weight between Chow and WD at 16 – week timepoint **(B)** Tibia Length between Chow and WD at 16 – week timepoint; Chow **(C)** Heart Weight/Tibia Length ratio between Chow and WD at 16-week timepoint; Chow: n = 11 WD: n= 10, unpaired t – test, *p<0.05

Figure 12 shows heart weights (A), tibia lengths (B), and heart weight/tibia length ratios (C) of chow or WD-fed mice after 16 weeks of the diet protocol. HW and HW/TL was significantly lower in WD-fed mice.

Table 8 Food Consumption over 16 weeks of Chow and WD - fed Ldlr$^{-/-}$ mice during 16 weeks of diet

Time (wks)	1	2	3	4	5	6	7	8	9	10	11	12	13	14	15	16
Chow	29,30 ± 1.11	29,00 ± 1.29	29,78 ± 1.26	29,38 ± 1.03	29,17 ± 1.13	29,77 ± 0.46	30,50 ± 0.57	33,37 ± 0.52	32,33 ± 1.34	30,55 ± 0.95	30,26 ± 0.76	29,51 ± 0.85	29,82 ± 1.35	29,67 ± 0.67	32,04 ± 0.93	36,28 ± 2.82
WD	22,7 ± 1.03	20,9 ± 0.67	21,6 ± 0.60	21,5 ± 0.54	20,9 ± 0.72	23,5 ± 1.02	23,5 ± 1.43	20,8 ± 0.82	21,3 ± 1.49	22,1 ± 1.86	22,1 ± 1.67	22,1 ± 1.38	22,0 ± 1.45	21,7 ± 1.24	20,7 ± 1.11	21,2 ± 1.25
Chow/WD	***	***	***	***	***	***	***	***	***	***	***	**	**	**	*	ns

Chow n = 11, WD n = 10, unpaired t – test, mean ± SEM, *p <0.05, ** p<0.01, ***p<0.001

Table 9 Water Consumption over 16 weeks of Chow and WD - fed Ldlr$^{-/-}$ mice during 16 weeks of diet

Time (wks)	1	2	3	4	5	6	7	8	9	10	11	12	13	14	15	16
Chow	30,0 ± 1.76	29,7 ± 2.16	30,1 ± 2.61	29,9 ± 2.19	28,9 ± 1.69	32,0 ± 2.09	37,1 ± 2.24	39,1 ± 4.14	39,4 ± 3.36	34,7 ± 2.44	34,5 ± 2.12	34,1 ± 2.71	33,6 ± 1.61	31,2 ± 2.16	42,6 ± 1.96	38,9 ± 3.46
WD	22,6 ± 1.00	21,9 ± 1.21	20,8 ± 1.86	23,0 ± 1.99	24,7 ± 4.52	23,8 ± 2.16	24,0 ± 1.58	22,9 ± 2.49	22,1 ± 2.33	20,8 ± 1.65	22,2 ± 1.16	21,4 ± 1.47	19,1 ± 0.74	21,1 ± 1.36	23,0 ± 1.97	29,4 ± 7.49
Chow/WD	***	***	***	***	***	***	***	***	***	***	***	**	**	*	ns	ns

Chow n = 11, WD n = 10, unpaired t – test, mean ± SEM,; *p <0.05, **p<0.01, ***p<0.001

Tables 8 and 9 show weekly measurements of food consumption and water consumption in chow-fed or WD-fed mice, respectively. At every time point between weeks 1-15, food consumption was lower in WD-fed mice. Similarly, water consumption was lower in the WD group at every time point between weeks 1-14.

14.1.1 Blood Glucose Tolerance Test

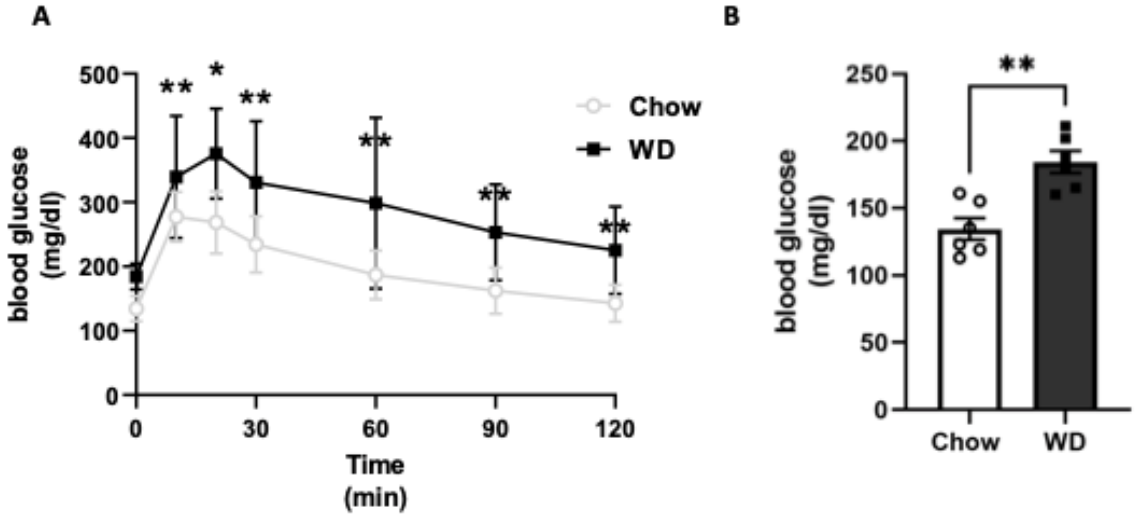

Figure 13: Blood glucose tolerance test in Chow and WD-fed Ldlr$^{-/-}$ mice after 16 weeks of diet

(A) Blood glucose levels in Chow vs. WD fed Ldlr$^{-/-}$ mice over 10, 20, 30, 60, 90 and 120 min after intravenous glucose challenge **(B)** Fasting blood glucose levels in Chow vs. WD fed Ldlr$^{-/-}$ mice after 16 weeks of diet before glucose challenge; n = 6; unpaired t – test, *p<0.05, **p<0.01

Figure 13 displays the results of glucose tolerance tests over 10, 20, 30, 60, 90 and 120 minutes after intravenous glucose challenge (A) and fasting blood glucose levels before the glucose challenge, after fasting 4-5 hours, (B) performed after 16 weeks of Chow or WD feeding. Blood glucose values were higher in WD-fed mice compared to chow-fed mice at all time points during the glucose tolerance test.

14.1.2 Echocardiography

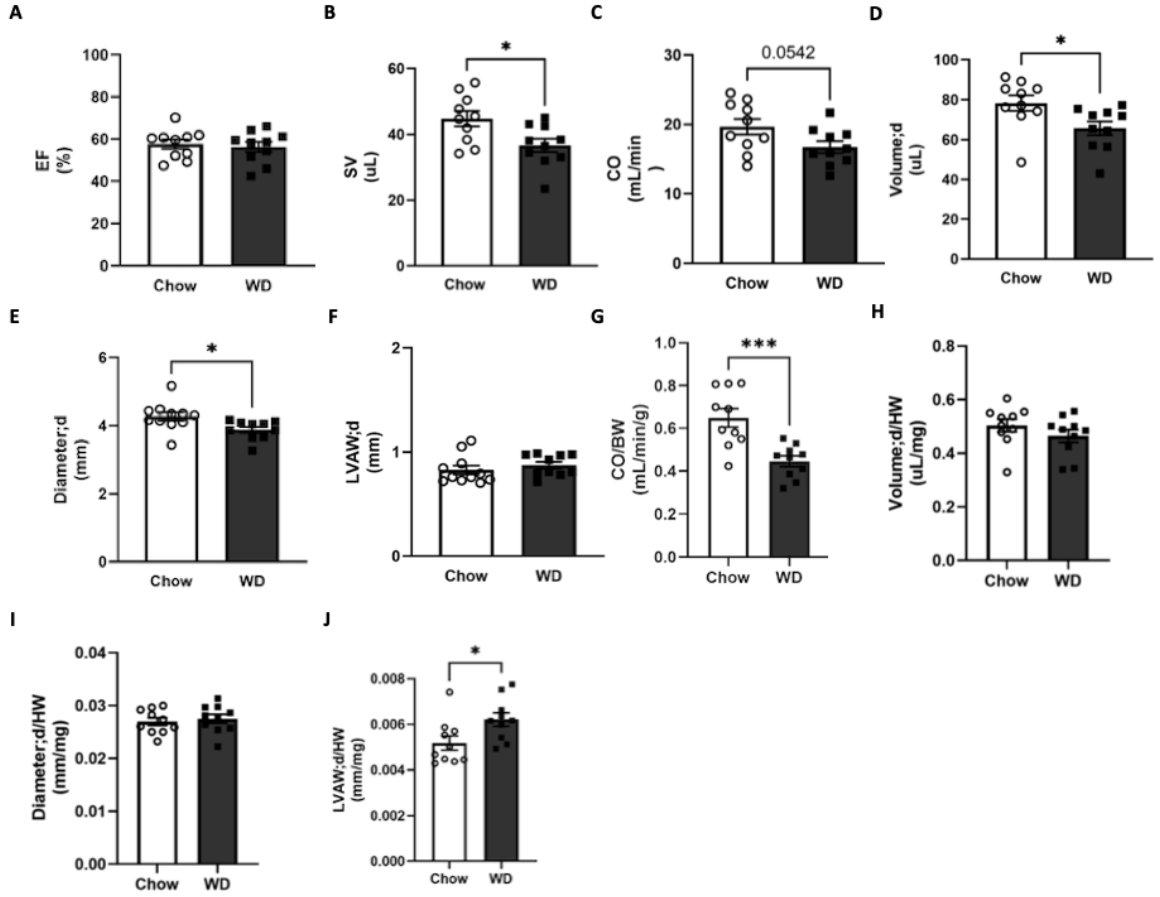

Figure 14: **Systolic Function and Remodeling in Chow and WD-fed Ldlr$^{-/-}$ mice after 16 weeks of diet:**

(A) Ejection Fraction in % **(B)** Stroke Volume in µL **(C)** Cardiac Output In µL/min **(D)** Volume in diastole in µL **(E)** Diameter in diastole in mm **(F)** Left ventricular anterior wall thickness in diastole in mm **(G)** Cardiac Output In µL/min normalized to Body Weight in g **(H)** Volume in diastole in µL normalized to Heart Weight in mg **(I)** Diameter in diastole in mm normalized to Heart Weight in mg **(J)** Left ventricular anterior wall thickness in diastole in mm normalized to Heart Weight in mm, Chow: n = 10, WD n = 10, unpaired t - test, * p < 0,05, ** p<0,01

Figure 14 shows parameters of cardiac function and structure measured by echocardiography in mice after 16 weeks of chow or WD feeding. Ejection fraction (EF) was not different between groups (Figure 15 A). Stroke volume was significantly lower in WD-fed mice (Figure 15 B), and cardiac output (CO) showed lower mean values in WD fed mice that did not quite reach statistical significance (Figure 15 C). When normalized to body weight, WD-fed animals had significantly lower cardiac output compared to standard chow-fed animals. (Figure G) Enddiastolic diameter and enddiastolic volume were significantly lower in WD-fed mice compared to chow-fed mice (Figures 15 D, E) whereas LV anterior wall thickness was not different between the groups (Figure 15 F). When normalized to heart weight, enddiastolic diameter and volume were unchanged between groups, whereas LV anterior wall thickness was increased in WD-fed mice (Figure H, I, J).

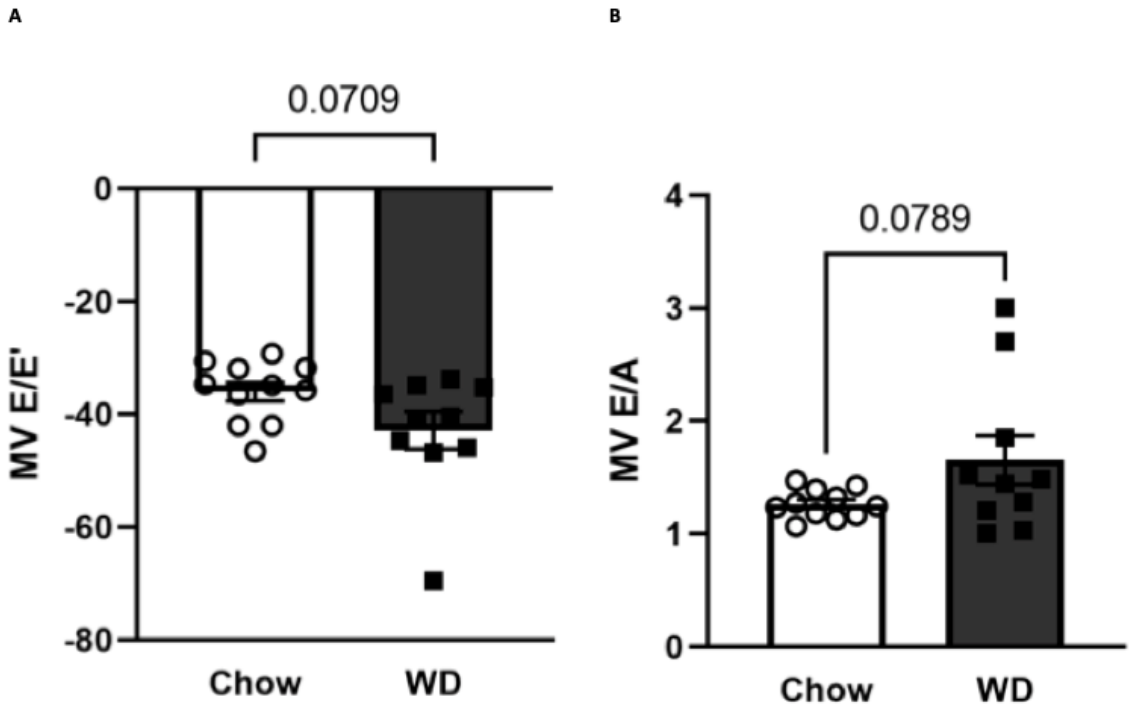

Figure 15: **Diastolic Function in Chow and WD-fed Ldlr$^{-/-}$ mice after 16 weeks of diet**

(A) MV E/E', **(B)** MV E/A); Chow: n = 11, WD group n = 10, unpaired t - test; * p < 0,05; ** p<0,01

Figure 15 shows MV E/E' and MV E/A ratios of chow or WD-fed mice measured after 16 weeks. Mean values of MV E/E' and MV E/A were lower in WD-fed mice compared to chow-fed mice although these decreases did not achieve statistical significance.

14.2 Histology

14.2.1 HE stain

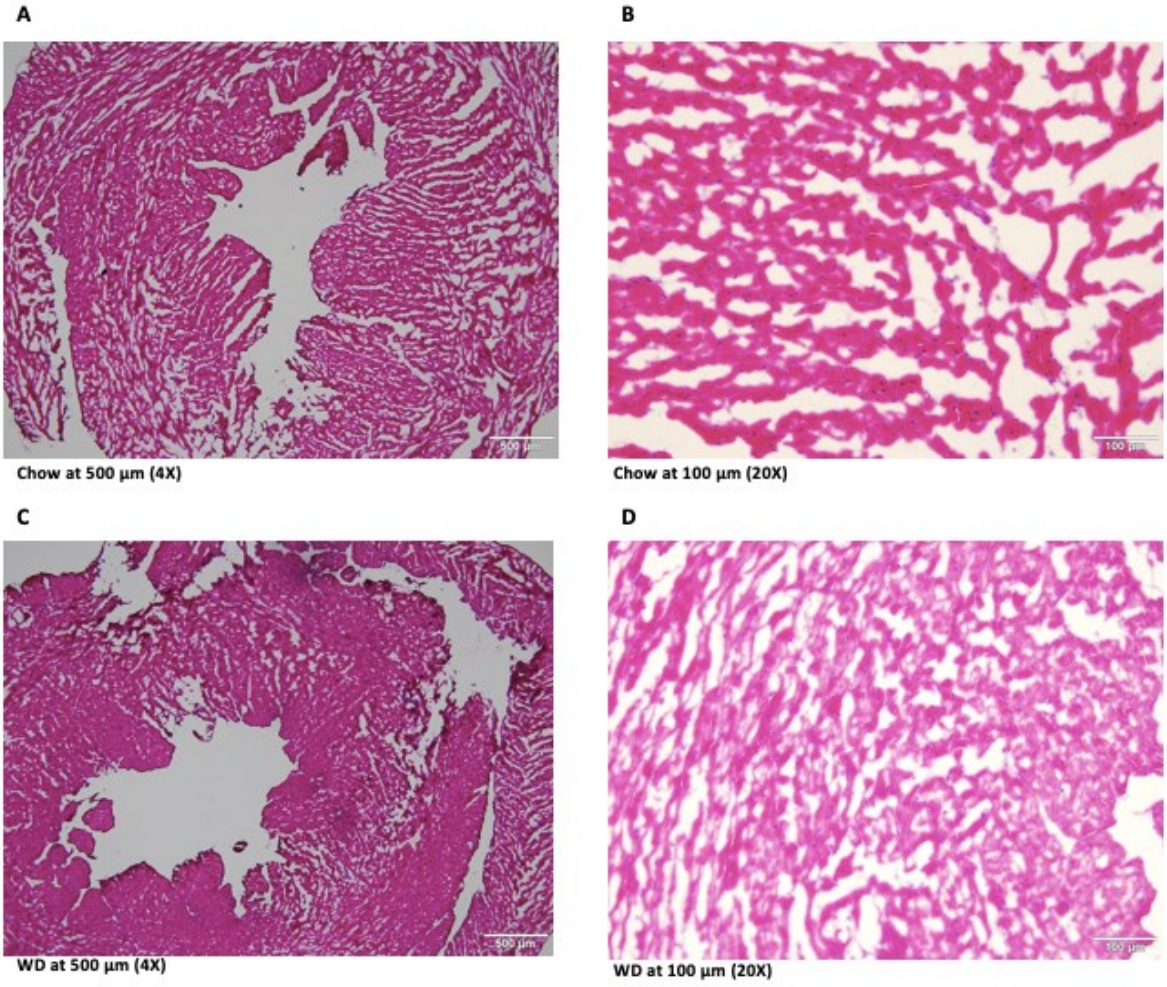

Figure 16: HE stain in Chow and WD-fed Ldlr$^{-/-}$ mice after 16 weeks of diet

(A) Overview Chow Group at 500 µm = 4X; **(B)** Detail View at 100 µm = 20X **(C)** Overview WD Group at 500 µm = 4X **(D)** Detail view at 100 µm = 20X

Figure 16 shows representative images of HE staining of the LV of chow-fed or WD-fed mice at different magnifications (4x or 20x). No gross morphological alterations were observed between the groups.

14.2.2 WGA stain

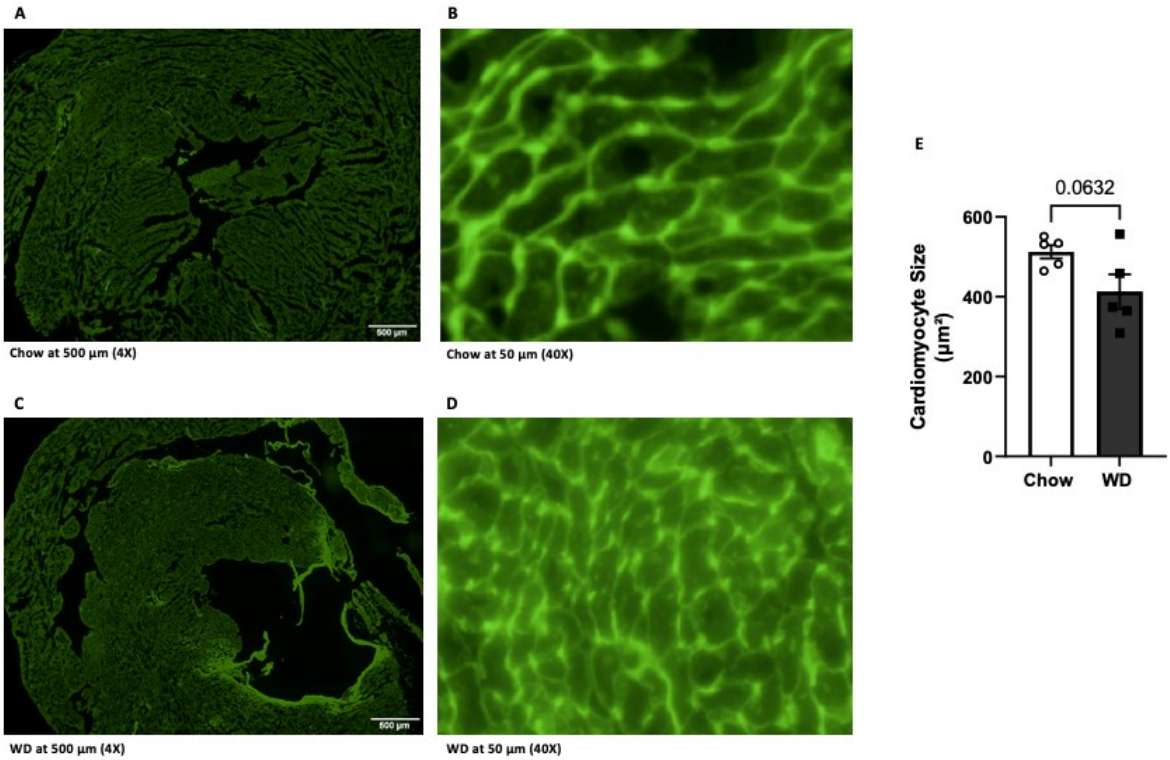

Figure 17: WGA stain in Chow and WD-fed Ldlr$^{-/-}$ mice after 16 weeks of diet

(A) Overview Chow Group at 500 µm = 4X; **(B)** Detail View at 100 µm = 40X **(C)** Overview WD Group at 500 µm = 4X **(D)** Detail view at 100 µm = 40X **(E)** Cardiomyocyte Size; Chow: n = 11, WD group n = 10, unpaired t - test; * p < 0,05; ** p<0,01

Figure 17 shows representative images of WGA staining of the LV of chow-fed or WD-fed mice at different magnifications (4x or 40x). Mean values of cardiomyocyte size were lower in WD-fed mice although statistical significance was not achieved.

14.2.3 Masson's trichrome stain

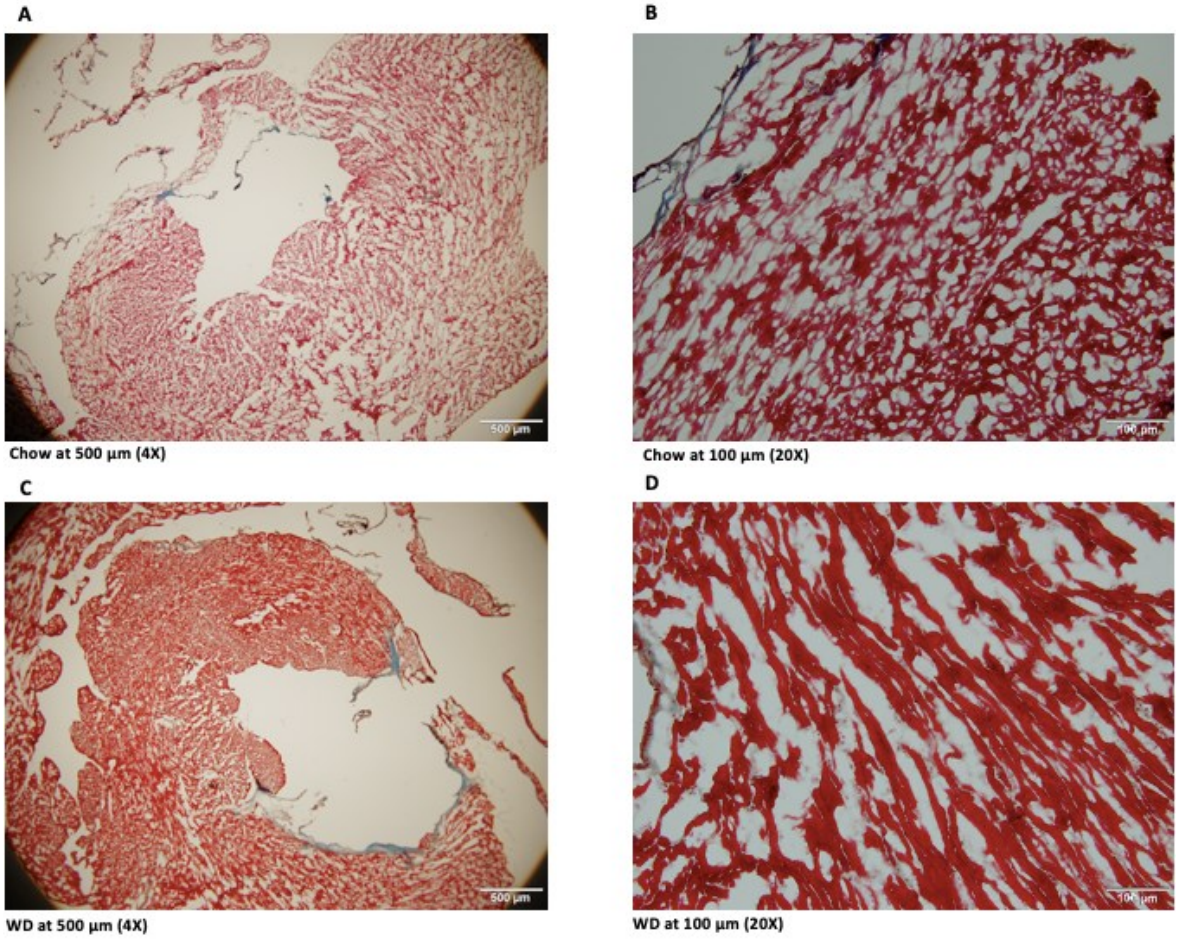

Figure 18: Masson's trichrome stain in Chow and WD-fed Ldlr$^{-/-}$ mice after 16 weeks of diet

(A) Overview Chow Group at 500 µm = 4X; **(B)** Detail View at 100 µm = 20X **(C)** Overview WD Group at 500 µm = 4X **(D)** Detail view at 100 µm = 20X

Figure 18 shows representative images of Masson's trichrome staining of the LV of chow-fed or WD-fed mice at different magnifications (4x or 20x). Using software-based quantification of the stain, no significant detection above background was detected in either group, indicating very low collagen content in hearts of chow or WD-fed mice, and indicating that significant fibrosis was absent in response to WD feeding.

15 Discussion

In this study the effects of obesity and T2DM on cardiac function and structure in a mouse model that also develops atherosclerosis were investigated. Using Ldlr$^{-/-}$ mice fed either normal chow or a Western diet for a duration of 16 weeks, it could be shown that WD lead to obesity and impaired glucose tolerance, decreased heart size despite increased body weight, increased LV wall thickness, lower cardiac output and a trend towards impaired E/A and E/E' ratio. From these data, we conclude that WD induced obesity and insulin resistance in Ldlr$^{-/-}$ mice as observed in other models of obesity, T2D, and metabolic syndrome. Body weight-driven gain of heart weight may be attenuated in this model while WD may induce hypertrophic cardiac remodeling and potentially diastolic dysfunction. Furthermore, smaller heart size may limit cardiac output of obese Ldlr$^{-/-}$ mice. Thus, this atherosclerosis-prone model of obesity and T2DM displays features of diabetic cardiomyopathy observed in other animal models that lack atherosclerosis. A detailed discussion follows below.

Our WD-fed mice had a significant increase in body weight during 16 weeks of feeding. Similar results were seen by Jiang et. al. (Jiang, 2005). They fed C57BL/6J mice a HFD, to study the impact of overweight on the development of kidney disease. The body weight of their experimental group was significantly increased than their control group. Furthermore, their mice also developed obesity, hyperglycemia and hyperinsulinemia. Another group that also confirmed our findings was Bostick et. al. They fed four-week-old C57BL6/J mice a High Fat/ High Fructose Western diet for 16 weeks intending to find the connection between obesity and heart disease expressed as early diastolic dysfunction in diseases such as metabolic cardiomyopathy. They also found a very significant difference between their WD group and their control group. (Bostick, 2014) Manrique and colleagues not only studied the impact of obesity and insulin resistance on early diastolic dysfunction after a WD but also looked at gender differences. In their experimental setup four–week–old C57BL6/J mice received 8 weeks of High Fat/ High Fructose WD feeding after which the body composition between sexes as well as a control group were compared. They found that not only diet-based but also between sexes their experimental group had a significant increase of body weight over the course of the feeding period. (Manrique, 2013) In conjunction with these results and our results, it can be concluded that feeding Ldlr$^{-/-}$ mice a WD over a longer period of time leads to a similar phenotype of overweight and obesity as observed in animal models lacking atherosclerosis.

Over the time of 120 minutes, all WD fed mice had significantly higher blood glucose levels at all time points. This has been shown in many experimental studies. One group who also did a glucose tolerance test in a Ldlr$^{-/-}$ model fed with WD but in a different context were Gosh et. al. They wanted to find the connection between kidney failure and known cardiovascular diseases. In their glucose tolerance test, which they did after 16 – weeks of study, they found a very significant increase in blood glucose levels in their WD group over the 120 minutes. (Ghosh, 2015). Another group that studied the role of a HFD and the development of diabetes mellitus was Yan et. al. After feeding 8-week-old C57BL/6 mice a HFD for 42 weeks they did a Glucose tolerance test. Similar to us they found a significant increase in blood glucose levels after 0, 30, 60, 90, 120 and 150 minutes, for their HFD group at all measuring points. (Che, 2018) Based on our data, these and probably many

other publications in literature we conclude that prolonged feeding of a WD leads to the development of impaired glucose tolerance in $Ldlr^{-/-}$ mice.

The latter conclusion is supported by the observation of a very significant increase in fasting blood glucose levels after 16 weeks of HFD in our study. In their publication about metabolic cardiomyopathy Bostick et. al also found a similar trend. WD fed mice had higher fasting glucose levels. However, although their results had a trend, they were not significant. (Bostick, 2014) In contrast, Mazumder et. al. who used 8-week ob/ob mice to study impaired cardiac efficiency and fatty acid oxidation under a standard chow found a significant increase in such. They did not need HFD or WD because ob/ob mice are known to develop insulin resistance and glucose intolerance due to genetic deficiency of leptin. After a six-hour fast, their ob/ob mice blood glucose levels were significantly increased. (Mazumber & Dale, 2004) Maurya et. al used eight-week-old C57BL/6 male mice which were fed a WD to explore the metabolic remodeling of the heart during impaired systolic function and reduced ejection fraction for 20, respectively 24 – weeks. The results of their study's fasting glucose levels which they did twice showed a very significant increase of fasting blood glucose levels in the WD group in both tests. (Maurya, 2023) Thus, although no reliable definitions exist to diagnose perturbations of glucose metabolism in animal models, the increase of fasting blood glucose levels in our study further support the development of impaired glucose tolerance.

Our study showed that a 16-week WD feeding period leads to a significant decrease in the heart weight to tibia length ratio. Bostick et. al. who in their previously mentioned publication fed four-week-old C57BL6/J mice a High Fat/ High Fructose Western diet for 16 weeks to induce diastolic dysfunction also looked at normalized heart weights. They found their experimental animals all had significantly increased heart weight to tibia length ratios. (Bostick, 2014) These findings could not be reproduced by Nguyen et. al. who used a WD to study the contribution of diet-induced obesity and T2DM to the development of cardiac dysfunction. In their experimental setup, they used 10 – 12 weeks old male C57BL/6J for a 12-week long feeding period. They did not observe a change in heart weight to tibia length ratios between their experimental groups using a WD and only a trend using what they specified as a high fat WD. Their results, however, also showed that if at all, heart weight to tibia length ratios in their experiments using a WD were increased. (Nguyen, 2017) Another group that studied the alteration of energy metabolism mechanisms of the heart caused by WD were Neves et. al. Although they used a different strain of mouse, a Swiss mouse, they observed similar results after a 16-week feeding period. Their experimental group, which was fed WD, had a significantly increased heart weight tibia length ratio. (Neves, 2014) Thus, our results of a decrease instead of an increase in heart weight to tibia length ratio are in contrast to other studies investigating models of obesity that do not develop atherosclerosis and may point towards an attenuation of weight gain associated growth of the heart in our model. Of note, while cardiomyocyte size was statistically unaltered in our study, WD fed mice showed a trend towards reduced cell size, thereby validating our observation of reduced heart size. A potential reason may be the development of cardiomyocyte insulin resistance. In fact, mice with cardiomyocyte-specific deletion of the insulin receptor as a model of cardiac insulin resistance demonstrated decreased heart and cardiomyocyte size (PMID 11877471). Thus, the development of systemic insulin resistance (based on impaired systemic glucose tolerance) in obesity in our

model, which may include cardiac insulin resistance, may potentially contribute to growth retardation of the heart despite an increase in body weight.

Clinically, the most important parameter for defining the presence of cardiac hypertrophy is an increase in LV wall thickness. Although heart size was decreased and cardiomyocyte size trended towards a decrease, LV wall thickness relative to heart weight was increased in our model, suggesting the presence of cardiac remodeling. This observation matches numerous reports from studies in animal models of obesity, insulin resistance and type 2 diabetes that observed cardiac remodeling and hypertrophy (reviewed in PMID: 35679363). Thus, overlapping mechanisms may cause a phenotype of growth retardation of the heart with simultaneous development of cardiac hypertrophy. The reasons for such a phenotype remain unclear and may require unbiased studies of the cardiac transcriptome and proteome for hypothesis generation in follow-up studies, e.g. using RNA sequencing and MS-based proteomics.

An additional observation during our echocardiographic studies was a decrease in stroke volume and cardiac output although ejection fraction remained unchanged. Such a constellation of parameters is consistent with the development of hypertrophic remodeling, in particular concentric hypertrophy, in which stroke volume and consequently cardiac output are decreased due to a smaller LV cavity, however the relative ejection of blood (as measured as ejection fraction) remains unaltered. Interestingly, Heinonen et. al. published a study in which they studied macrovascular diabetic complications in 18–month–old Ldlr $^{-/-}$ mice which received a Western diet for three months. They found a significant decrease in ejection fraction, but also in left ventricular wall thickness in diastole and LV volume during diastole in their experimental group (Heinonen, 2011). While these findings seem to be consistent with a much more pronounced phenotype compared to our phenotype, this may reflect a progression towards heart failure which may result from decompensation of pathological cardiac hypertrophy and remodeling. Given that these mice were much older compared to our study, it needs to be considered that these heart may be much more susceptible to detrimental stimuli such as a WD and may thus suffer a stronger impairment of cardiac function and remodeling despite a similar period of WD feeding. On the other side, Delemasure et. al. conducted a study in which the impact of a HFD on the plasma antioxidant status and cardiac function was investigated in female Ldlr $^{-/-}$ mice. They fed adult female C57BL/6J mice a HFD for 17 weeks. They found a significantly increased ejection fraction and an unchanged cardiac output after a HFD in their experimental group. (Delemasure, 2012) The latter results imply that numerous factors may clearly impact the development of the cardiac phenotype in response to a dietary treatment, including sex, genetic phenotype, composition of the diet (WD versus HFD), duration of diet, age of the animal, and potentially housing conditions (including various components of stress in housing facilities).

We observed a trend towards a decrease for MV E/E', suggesting that WD may have induced diastolic dysfunction in Ldlr$^{-/-}$ mice. Another group that studied diastolic function were Tang et. al. who published a paper about arterial stiffness as predictor of atherosclerosis. They fed 8-week-old male *ApoE*$^{-/-}$ mice a HFD for 8 weeks. During their study they evaluated cardiac function using echocardiography every 4 weeks. Before sacrifice they found significantly increased MV E/A ratio as well as MV E/E' ratio indicating diastolic dysfunction. (Tang M. , 2021) Similar results were seen by Bostick et. al. who

studied whether a mineralcorticoid receptor blockade can prevent diet – induced diastolic dysfunction in female mice. For their study, they used three-week-old C57BL6J female mice and fed them a WD for 16 weeks. They also found impaired diastolic function indicated by a significant decrease in the MV E/A ratio but no difference in MV E/E' ratios. (Bostick, 2014) In light of these publications, we conclude that diet-induced obesity and the development of a prediabetic state may indeed contribute to the development of diastolic dysfunction in the heart. These findings thereby support the clinical observation of a high prevalence of diastolic heart failure (or HFpEF) in individuals suffering long-term type 2 diabetes or metabolic syndrome.

In the present study, a 16-week WD feeding period did not lead to any difference in cardiac fibrosis when evaluated by Masson's trichrome staining. This finding is important because Tan et. al identified cardiac fibrosis as one of the cardinal features of DbCM. (Tan Y. , 2020) Importantly, Tikellis et. al. compared C57BL6J and *RAGE* knockout mice under a standard chow and a WD for 16 weeks. After sacrifice, they used multiple methods to detect cardiac fibrosis. Similar to our results, no increase in fibrosis was visible using histology. However, they found that gene expression for collagen I and collagen IV was significantly increased indicative of ongoing fibrosis development. (Tikellis, 2008) Hongkai et. al. studied myocardial interstitial fibrosis as a driving factor in DbCM. In their study, they used 8-week-old C57Bl/6J male mice that were fed normal chow but were injected intraperitoneally with STZ. Every four weeks of their study three mice were sacrificed to examine the progression of myocardial interstitial fibrosis. After 12 weeks they found a significant increase in fibrosis in their experimental group. (Hongkai, 2022) Taken together, we were unable to demonstrate an increase in fibrosis by histology in WD-fed mice, however, it seems reasonable to speculate that the method was not sensitive enough to detect early fibrotic remodeling in these hearts. Future studies should investigate the expression of collagens in these mice.

A limitation of this study is that it attempts to characterize a complex disease such as DbCM only with a limited amount of methods. For this reason, the interpretation of the experimental data can only be fundamentally incomplete. Additional in-depth studies on cardiac function and morphology, paralleled by studies aiming at elucidating underlying molecular mechanisms, are warranted. Looking into the future, we can summarize that it will probably take a lot more work in basic research on DbCM to understand the underlying processes. However, based on the rising incidence of obesity and type 2 diabetes, understanding this increasingly recognized cardiac entity and potentially developing suitable therapies are challenges that need to be faced to improve medical treatment for this population at high risk for cardiac complications.

16 Bibliography

Aasum, E. (February. 1 2003). *Age-dependent changes in metabolism, contractile function, and ischemic sensitivity in hearts from db/db mice*. Von Diabetes Journal: https://diabetesjournals.org/diabetes/article/52/2/434/26759/Age-Dependent-Changes-in-Metabolism-Contractile abgerufen

Aasum, E. (2006, February 1). *Increased myocardial oxygen consumption reduces cardiac efficiency in diabetic mice.* Retrieved from Diabetes Journals: https://diabetesjournals.org/diabetes/article/55/2/466/12670/Increased-Myocardial-Oxygen-Consumption-Reduces

Aneja, T. (2008, September 9). *The American Journal of Medicine.* Retrieved from https://www.sciencedirect.com/science/article/abs/pii/S0002934308004713

Anker. (2021, October 2021). *Empagliflozin in heart failure with a preserved ejection fraction*. Retrieved from The New England Journal of Medicine: https://www.nejm.org/doi/full/10.1056/NEJMoa2107038

Bajai, A. (2018, November 1). *The Role of Leukocytes in Diabetic Cardiomyopathy*. Retrieved from Frontiers in Phyiology: https://www.frontiersin.org/journals/physiology/articles/10.3389/fphys.2018.01547/full

Bartolomaeus, H. (2019, March 12). *Short-Chain Fatty Acid Propionate Protects From Hypertensive Cardiovascular Damage*. Retrieved from American Heart Association: https://pubmed.ncbi.nlm.nih.gov/30586752/

Berg, K. (July 2002). *Spontaneous atherosclerosis in the proximal aorta of LPA transgenic mice on a normal diet*. Von Atherosclerosis: https://www.atherosclerosis-journal.com/article/S0021-9150(01)00772-9/abstract abgerufen

Bjorklund, M. (2014, March 27). *Induction of atherosclerosis in mice and hamsters without germline genetic engineering*. Retrieved from Circulation: https://www.ahajournals.org/doi/10.1161/circresaha.114.302937

Bolli, B. M. (2004, July 2004). *Myocardial Protection at a Crossroads.* Retrieved from Circulation Research: https://www.ahajournals.org/doi/10.1161/01.res.0000137171.97172.d7

Boly, C. (2016, September 20). *The effect of perioperative insulin treatment on cardiodepression in mild adiposity in mice*. Retrieved from Cardiovascular Diabetology: https://cardiab.biomedcentral.com/articles/10.1186/s12933-016-0453-y

Bostick, B. (2014). Dipeptidyl peptidase inhibition prevents diastolic dysfunction and reduces myocardial fibrosis in a mouse model of Western diet induced obesity. *Metabolism*, 1000-1011. Retrieved from Metabolism: https://www.sciencedirect.com/science/article/abs/pii/S0026049514001103

Bostick, B. (2014, March 15). *Mineralocorticoid receptor blockade prevents Western diet-induced diastolic dysfunction in female mice*. Retrieved from American Journals of Physiology: https://journals.physiology.org/doi/prev/20150307-aop/abs/10.1152/ajpheart.00898.2014

Boudina. (2005, October 5). *Reduced Mitochondrial Oxidative Capacity and Increased Mitochondrial Uncoupling Impair Myocardial Energetics in Obesity*. Retrieved from Circulation: https://www.ahajournals.org/doi/10.1161/circulationaha.105.554360

Boudina, A. (2007, Jun 26). *Circulation Research.* Retrieved from https://www.ahajournals.org/doi/full/10.1161/CIRCULATIONAHA.106.679597

Braczko, A. (2022, September 23). *Cardiac Mitochondria Dysfunction in Dyslipidemic Mice*. Retrieved from Journal of Molecular Sciences: https://www.researchgate.net/publication/364031482_Cardiac_Mitochondria_Dysfunction_in_Dyslipidemic_Mice

Brahma, M. (2020, July 30). *Increased Glucose Availability Attenuates Myocardial Ketone Body Utilization*. Retrieved from Journal of the American Heart Association: https://www.ahajournals.org/doi/full/10.1161/JAHA.119.013039

Braunwald. (1971, January 1). *Factors Influencing Infarct Size Following Experimental Coronary Artery Occlusions.* Retrieved from Circulation: https://www.ahajournals.org/doi/10.1161/01.CIR.43.1.67

Breslow, J. (n.d.). *Jackson Laboratory*. Retrieved May 29, 2023, from https://www.jax.org/strain/006580

Brosius, F. (2005, January 16). *Mouse models of diabetic nephropathy*. Retrieved from Journals of American Society of Nephrology: https://journals.lww.com/jasn/fulltext/2009/12000/mouse_models_of_diabetic_nephropathy.8.aspx

Brunvand, L. (2017, May 25). *Advanced glycation end products in children with type 1 diabetes and early reduced diastolic heart function*. Retrieved from BMC Cardiovascular Disorders: https://bmccardiovascdisord.biomedcentral.com/articles/10.1186/s12872-017-0551-0

Buchanan, J. (2005, December 1). *Reduced Cardiac Efficiency and Altered Substrate Metabolism Precedes the Onset of Hyperglycemia and Contractile Dysfunction in Two Mouse Models of Insulin Resistance and Obesity*. Retrieved from Endocrinology: https://academic.oup.com/endo/article/146/12/5341/2500472

Bugger, D. (2014, January 30). *Diabetologia.* Retrieved from https://www.ncbi.nlm.nih.gov/pmc/articles/PMC3969857/#:~:text=Multiple%20molecular%20mechanisms%20act%20in,Altered%20metabolism%20and%20mitochondrial%20dysfunction

Bugger, H, Byrne, N, Abel, & D. (2022, June 10). *Animal Models of Dysregulated Cardiac Metabolism.* Retrieved from Circulation Research: https://www.ahajournals.org/doi/10.1161/CIRCRESAHA.122.320334

Bugger, H. (May 2012). *Genetic loss of insulin receptors worsens cardiac efficiency in diabetes*. Von Journal of Molecular Cellular Cardiology: https://www.sciencedirect.com/science/article/pii/S0022282812000570 abgerufen

Bugger, H. (2016, Juni 13). Mitochondrial sirtuins in the heart. *Heart Failure Reviews*, pp. 2-3.

Bugger, H. (2022, June 9). *Animal Models of Dysregulated Cardiac Metabolism*. Retrieved from Circulation: https://www.ahajournals.org/doi/10.1161/CIRCRESAHA.122.320334?url_ver=Z39.88-2003&rfr_id=ori:rid:crossref.org&rfr_dat=cr_pub%20%200pubmed

Cai, L. (2001, September). *Oxidative stress and diabetic cardiomyopathy: a brief review*. Retrieved from Cardiovascular Toxicology: https://link.springer.com/article/10.1385/CT:1:3:181

Callow, M. (3. September 1995). *Atherogenesis in transgenic mice with human apolipoprotein B and lipoprotein(a)*. Von Journal of Clinical Investigations: https://dm5migu4zj3pb.cloudfront.net/manuscripts/118000/118203/JCI95118203.pdf abgerufen

CDC. (2023). *Centers for Disease Control and Prevention National Diabetes Statistics Report*. Retrieved from https://www.cdc.gov/diabetes/data/statistics-report/index.html?CDC_AA_refVal=https%3A%2F%2Fwww.cdc.gov%2Fdiabetes%2Fdata%2Fstatistics%2Fstatistics-report.html

Centner, A. (2024, June 29). *High-Fat Diet Augments Myocardial Inflammation and Cardiac Dysfunction in Arrhythmogenic Cardiomyopathy*. Retrieved from Nutrients: https://www.researchgate.net/publication/381911451_High-Fat_Diet_Augments_Myocardial_Inflammation_and_Cardiac_Dysfunction_in_Arrhythmogenic_Cardiomyopathy

Che, Y. (2018, September 18). *Role of autophagy in a model of obesity: A long-term high fat diet induces cardiac dysfunction*. Retrieved from Molecular Medicine Reports: https://pubmed.ncbi.nlm.nih.gov/30066870/

Chiao. (2021, August 21). *Circulation Heart Failure*. Retrieved from NAD+ Redox Imbalance in the Heart Exacerbates Diabetic Cardiomyopathy: https://www.ahajournals.org/doi/10.1161/CIRCHEARTFAILURE.120.008170

Chiao, Y. (2021, August 21). *NAD+ Redox Imbalance in the Heart Exacerbates Diabetic Cardiomyopathy*. Retrieved from American Heart Journals: https://www.ahajournals.org/doi/10.1161/CIRCHEARTFAILURE.120.008170

Clinical trials. (2021, July 14). Retrieved from https://clinicaltrials.gov/study/NCT03151239

Cohn. (6. December 2001). *A Randomized Trial of the Angiotensin-Receptor Blocker Valsartan in Chronic Heart Failure*. Von The New England Journal of Medicine: https://www.nejm.org/doi/full/10.1056/nejmoa010713 abgerufen

Colberg. (2010, December 1). *Exercise and Type 2 Diabetes: The American College of Sports Medicine and the American Diabetes Association: joint position statement*. Retrieved from Diabetes Journals: https://diabetesjournals.org/care/article/33/12/e147/39268/Exercise-and-Type-2-DiabetesThe-American-College

Consentino, G. B. (2020, July 01). *European Heart Journal.* Retrieved from https://doi.org/10.1093/eurheartj/ehz486

Cruz, L. (2017, June 2). *Nitric Oxide Signaling in Heart Failure With Preserved Ejection Fraction*. Retrieved from Journal of the American College of Cardiology: https://www.jacc.org/doi/abs/10.1016/j.jacbts.2017.05.004

Csabe, M. (2016, December 19). *Prevention of the development of heart failure with preserved ejection fraction by the phosphodiesterase-5A inhibitor vardenafil in rats with type 2 diabetes*. Retrieved from European Journal of Heart Failure: https://onlinelibrary.wiley.com/doi/full/10.1002/ejhf.711

Cui, M. (2013, May 12). *Chronic Caloric Restriction and Exercise Improve Metabolic Conditions of Dietary-Induced Obese Mice in Autophagy Correlated Manner without Involving AMPK*. Retrieved from Journal of Diabetes Research: https://onlinelibrary.wiley.com/doi/10.1155/2013/852754

Dandamudi S, S. J. (2014, February 26). *Journal of Cardiac Failure.* Retrieved from https://onlinejcf.com/article/S1071-9164(14)00078-5/fulltext

Delemasure, S. (2012, May 29). *Impact of high-fat diet on antioxidant status, vascular wall thickening and cardiac function in adult female LDLR–/– mice*. Retrieved from World Journal of Cardiovascular Diseases: https://www.scirp.org/html/14-1910055_21241.htm#ref40

Dempsey. (2016, October 3). *Sitting Less and Moving More: Improved Glycaemic Control for Type 2 Diabetes Prevention and Managemen*. Retrieved from Current Diabetes Reports: https://link.springer.com/article/10.1007/s11892-016-0797-4

Denis, M. (2012, January 18). *Gene inactivation of proprotein convertase subtilisin/kexin type 9 reduces atherosclerosis in mice*. Retrieved from Circulation: https://www.ahajournals.org/doi/full/10.1161/circulationaha.111.057406

Dhalla, N. (4. April 1978). *Subcellular basis of cardiac contractile failure.* Von Journal of Molecular and Cellular Cardiology: https://www.sciencedirect.com/science/article/abs/pii/002228287890384X abgerufen

Dinh, W. (2009, November 12). *Elevated plasma levels of TNF-alpha and interleukin-6 in patients with diastolic dysfunction and glucose metabolism disorders*. Retrieved from Cardiocasvular Diabetology: https://cardiab.biomedcentral.com/articles/10.1186/1475-2840-8-58

Dong, F. (2005, October 18). *Impaired cardiac contractile function in ventricular myocytes from leptin-deficient ob/ob obese mice*. Retrieved from Journal of Enocrinology: https://joe.bioscientifica.com/view/journals/joe/188/1/1880025.xml

Duncan, J. (2011, July). *Mitochondrial dysfunction in diabetic cardiomyopathy*. Retrieved from Mollecular Cell Research: https://www.sciencedirect.com/science/article/pii/S016748891100022X

Feng. (2010, January 26). *Diabetes/Metabolism Research and Reviews.* Retrieved from https://pubmed.ncbi.nlm.nih.gov/20013939/

Franssen, C. (2016, April 4). *Myocardial Microvascular Inflammatory Endothelial Activation in Heart Failure With Preserved Ejection Fraction*. Retrieved from Journal of American College of Cardiology: https://www.jacc.org/doi/abs/10.1016/j.jchf.2015.10.007

Frustaci, K. (2000). *Circulation Research*. Retrieved from https://www.ahajournals.org/doi/full/10.1161/01.RES.87.12.1123

FUJIFILM VisualSonics, Inc. (n.d.). *Visualsonics.* Retrieved from www.visualsonics.com

Fukai T, U.-F. M. (2011, June 6). *Antioxidans Redox Signaling.* Retrieved from https://pubmed.ncbi.nlm.nih.gov/21473702/

Fukamizu. (2022, August 24). *Nature.* Retrieved from Safety evaluation of β-nicotinamide mononucleotide oral administration in healthy adult men and women: https://www.nature.com/articles/s41598-022-18272-y

Galderisi, M. (2005, April 4). *Journal of Cardiovascular Ultrasound.* Retrieved from Journal of Cardiovascular Ultrasound: https://cardiovascularultrasound.biomedcentral.com/articles/10.1186/1476-7120-3-9

Gazewood, J. (2017, November 1). *American Family Physician.* Retrieved from American Family Physician: https://www.aafp.org/pubs/afp/issues/2017/1101/p582.html#diagnosis

Ge, F. (2010, October 1). *Insulin- and leptin-regulated fatty acid uptake plays a key causal role in hepatic steatosis in mice with intact leptin signaling but not in ob/ob or*

db/db mice. Retrieved from American Journal of Physiology: https://journals.physiology.org/doi/full/10.1152/ajpgi.00434.2009

Getz. (2012, March 1). *Animal Models of Atherosclerosis*. Retrieved from Atheriosclerosis, Thrombosis, Vascular Biology: https://www.ahajournals.org/doi/full/10.1161/ATVBAHA.111.237693

Getz, G. (1. May 2012). *Animal models of atherosclerosis*. Von Ateriosclerosis, Thrombosis Vascular Biology: https://www.ahajournals.org/doi/10.1161/ATVBAHA.111.237693 abgerufen

Ghosh, S. (2015, November 2015). *High Fat High Cholesterol Diet (Western Diet) Aggravates Atherosclerosis, Hyperglycemia and Renal Failure in Nephrectomized LDL Receptor Knockout Mice: Role of Intestine Derived Lipopolysaccharide*. Retrieved from Public Library of Science: https://journals.plos.org/plosone/article?id=10.1371/journal.pone.0141109

Ghuanghong, J. (2015, Dezember 18). *Nature Reviews Endocrinology.* Retrieved from Nture Reviews Endocrinology: https://www.nature.com/articles/nrendo.2015.216

Giacco, F. (29. October 2010). *Oxidative stress and diabetic complications*. Von Circulation: https://www.ahajournals.org/doi/abs/10.1161/CIRCRESAHA.110.223545 abgerufen

Gistera. (2022, June 9). *Animal Models of Atherosclerosis–Supportive Notes and Tricks of the Trade*. Retrieved from Circulation Research: https://www.ahajournals.org/doi/10.1161/CIRCRESAHA.122.320263

Gistera, A. (2022, June 9). *Animal Models of Atherosclerosis–Supportive Notes and Tricks of the Trade*. Retrieved from Circulation Research: https://www.ahajournals.org/doi/10.1161/CIRCRESAHA.122.320263

Golfouroush. (2020, November 30). *Mouse models of atherosclerosis and their suitability for the study of myocardial infarction*. Retrieved from Basic Research in Cardiology: https://www.researchgate.net/publication/346542008_Mouse_models_of_atherosclerosis_and_their_suitability_for_the_study_of_myocardial_infarction

Gräbner, R. (2009, January 12). *Lymphotoxin beta receptor signaling promotes tertiary lymphoid organogenesis in the aorta adventitia of aged ApoE-/- mice*. Retrieved from Journal of Experimental Medicine: https://rupress.org/jem/article/206/1/233/54206/Lymphotoxin-receptor-signaling-promotes-tertiary

Gu, J. (November 2016). *Diabetes*. Von Diabetes: https://www.researchgate.net/publication/311348272_Metallothionein_Is_Downstream_of_Nrf2_and_Partially_Mediates_Sulforaphane_Prevention_of_Diabetic_Cardiomyopathy abgerufen

Guarente, L. (2006, December 1). *Unlocking the Secrets of Longevity Lenes.* Retrieved from Scientific American: https://www.scientificamerican.com/article/unlocking-the-secrets-of-longevity/

Hölscher, B. B. (2016, October 26). *Internal Journal Molecular Sciences.* Retrieved from https://www.mdpi.com/1422-0067/17/12/2136

Hafstad, A. (2006, May 1). *Perfused hearts from Type 2 diabetic (db/db) mice show metabolic responsiveness to insulin*. Retrieved from American Journal of Physiology: https://journals.physiology.org/doi/10.1152/ajpheart.01063.2005

Hall, J. (1996, December 1). *Impaired pyruvate oxidation but normal glucose uptake in diabetic pig heart during dobutamine-induced work*. Retrieved from American Journal of Physiology: https://journals.physiology.org/doi/abs/10.1152/ajpheart.1996.271.6.H2320

Hartvigsen, K. (2007, January 25). *A diet-induced hypercholesterolemic murine model to study atherogenesis without obesity and metabolic syndrome*. Retrieved from Atherosclerosis, Thrombosis and Vascular Biology: https://www.ahajournals.org/doi/full/10.1161/01.ATV.0000258790.35810.02

Hasselbaink, D. (2003, May 1). *Ketone bodies disturb fatty acid handling in isolated cardiomyocytes derived from control and diabetic rats*. Retrieved from Biochemical Journal: https://portlandpress.com/biochemj/article-abstract/371/3/753/40692/Ketone-bodies-disturb-fatty-acid-handling-in

Hattori, Y. (2000, August 15). *Diminished function and expression of the cardiac Na+-Ca2+ exchanger in diabetic rats: implication in Ca2+ overload*. Retrieved from Journal of Physiology: https://www.researchgate.net/publication/12376960_Diminished_function_and_expression_of_the_cardiac_Na-Ca2_exchanger_in_diabetic_rats_Implication_in_Ca2_overload

Hayat, S., & Patel, B. (2004, November 24). *Clinical science.* Retrieved from Clinical science: https://portlandpress-1com-10013b5330a29.han.medunigraz.at/clinsci/article/107/6/539/67949/Diabetic-cardiomyopathy-mechanisms-diagnosis-and

Heerebeek, L. (2007, December 10). *Diastolic Stiffness of the Failing Diabetic Heart Importance of Fibrosis, Advanced Glycation End Products, and Myocyte Resting Tension*. Retrieved from Circulation: https://www.ahajournals.org/doi/full/10.1161/circulationaha.107.728550

Heinonen, S. (2011, June 30). *Cardiovascular Left ventricular dysfunction with reduced functional cardiac reserve in diabetic and non-diabetic LDL-receptor deficient apolipoprotein B100-only mice*. Retrieved from Cardiovascular Diabetology: https://cardiab.biomedcentral.com/articles/10.1186/1475-2840-10-59

Herbert, B. (2010, May 6). *Increased secretion of lipoproteins in transgenic mice expressing human D374Y PCSK9 under physiological genetic control*. Retrieved from American Heart Association: https://www.ahajournals.org/doi/10.1161/atvbaha.110.204040

Hobbs, H. (1990, January 1). *The LDL receptor locus in familial hypercholesterolemia: mutational analysis of a membrane protein*. Retrieved from Annual Reviews of Genetics: https://www.annualreviews.org/content/journals/10.1146/annurev.ge.24.120190.001025

Hongkai, Z. (2022, April 18). *Quantification of Early Diffuse Myocardial Fibrosis Through 7.0 T Cardiac Magnetic Resonance T1 Mapping in a Type 1 Diabetic Mellitus Mouse Model*. Retrieved from Journal of Magnetic Resonance Imaging: https://onlinelibrary.wiley.com/doi/10.1002/jmri.28207

Horn, A. (2015, July). *Cardiac Physiology of Aging: Extracellular Considerations* . Retrieved from Comprehensive Physiology: https://www.researchgate.net/publication/279726849_Cardiac_Physiology_of_Aging_Extracellular_Considerations

How, O. (2006, February 1). *Increased Myocardial Oxygen Consumption Reduces Cardiac Efficiency in Diabetic Mice*. Retrieved from Diabetes Journals: https://diabetesjournals.org/diabetes/article/55/2/466/12670/Increased-Myocardial-Oxygen-Consumption-Reduces

Hoxhaj, L. T. (2019, March 8). *https://www.science.org/doi/10.1126/science.aau3903.* Retrieved from https://www.science.org/doi/10.1126/science.aau3903

Hsu CP, H. N. (2009, November 16). *Autophagy.* Retrieved from https://www.tandfonline.com/doi/abs/10.4161/auto.5.8.10275

Hsu, H. (2015, September 10). *High-fat diet induces cardiomyocyte apoptosis via the inhibition of autophagy*. Retrieved from European Journal of Nutrition: https://link.springer.com/article/10.1007/s00394-015-1034-7

Ido, Y. (2007). *Antioxid Redox Signal*. Retrieved from Antioxidants Redox Signaling: https://www.liebertpub.com/toc/ars/12/1

Ishibashi S, H. R. (1993, August 1). *Journal of Clinical Investigation.* Retrieved from https://www.jci.org: https://www.jci.org/articles/view/116663

Ishibashi, S. (1. August 1993). *Hypercholesterolemia in low density lipoprotein receptor knockout mice and its reversal by adenovirus-mediated gene delivery*. Von Journal of Clinical Investigation: https://www.jci.org/articles/view/116663 abgerufen

Ishibashi, S. (1993, August 1). *Hypercholesterolemia in low density lipoprotein receptor knockout mice and its reversal by adenovirus-mediated gene delivery*. Retrieved from Journal of Clinical Investigaton: https://www.jci.org/articles/view/116663

Jiang, T. (2005, January 21). *Diet-induced Obesity in C57BL/6J Mice Causes Increased Renal Lipid Accumulation and Glomerulosclerosis via a Sterol Regulatory Element-binding Protein-1c-dependent Pathway*. Retrieved from Journal of Biological Chemistry: https://www.jbc.org/article/S0021-9258(20)79207-0/pdf

Kennedy. (2010, April 3). *Mouse models of the metabolic syndrome*. Retrieved from Disease Models and Mechanisms: https://pubmed.ncbi.nlm.nih.gov/20212084/

Kenny, H. (2019, January 4). *Heart failure in type 2 diabetes mellitus*. Retrieved from Circulation Research: https://www.ahajournals.org/doi/10.1161/CIRCRESAHA.118.311371

Kove, T. (2008, January 1). *Mitochondrial overload and incomplete fatty acid oxidation contribute to skeletal muscle insulin resistance*. Retrieved from Cell Metabolism: https://europepmc.org/article/med/18177724

Kozarsky, K. (1. March 2000). *Gene transfer and hepatic overexpression of the HDL receptor SR-BI reduces atherosclerosis in the cholesterol-fed LDL receptor-deficient mouse*. Von Atheriosclerosis, Thrombosis and Vascular Biology: https://www.ahajournals.org/doi/10.1161/01.ATV.20.3.721 abgerufen

Kury, L. (2018, April 10). *Calcium Signaling in the Ventricular Myocardium of the Goto-Kakizaki Type 2 Diabetic Rat*. Retrieved from Journal of Diabetes Research: https://www.hindawi.com/journals/jdr/2018/2974304/

Laroumanie, F. (2014, May 27). *CD4+ T cells promote the transition from hypertrophy to heart failure during chronic pressure overload*. Retrieved from Circulation: https://www.ahajournals.org/doi/10.1161/CIRCULATIONAHA.113.007101

Lawn, R. (17. December 1992). *Atherogenesis in transgenic mice expressing human apolipoprotein(a)*. Von Nature: https://www.nature.com/articles/360670a0 abgerufen

Leiva, A. (2011, July 11). *Mechanisms regulating hepatic SR-BI expression and their impact on HDL metabolism*. Retrieved from Atherosclerosis: https://www.atherosclerosis-journal.com/article/S0021-9150(11)00471-0/abstract

Lindstrom, P. (2007, May 29). *The physiology of obese-hyperglycemic mice [ob/ob mice]*. Retrieved from The Scientific World Journal: https://www.researchgate.net/publication/6217677_The_Physiology_of_Obese-Hyperglycemic_Mice_obob_Mice

Ling H, F. L. (2021, January 12). *Cardiovascular Toxicology.* Retrieved from https://pubmed.ncbi.nlm.nih.gov/33438065/

Lowes. (2004, August 16). *Effects of carvedilol on left ventricular mass, chamber geometry, and mitral regurgitation in chronic heart failure* . Retrieved from The American Journal of Cardiology: https://www.ajconline.org/article/S0002-9149(99)00059-4/pdf

Lundbaek, K. (1954, Februar 1954). *The Lancet.* Retrieved from https://www.sciencedirect.com/science/article/abs/pii/S0140673654909241

Luptak, I. (2019, July 17). *Energetic Dysfunction Is Mediated by Mitochondrial Reactive Oxygen Species and Precedes Structural Remodeling in Metabolic Heart Disease*. Retrieved from Antioxidants & Redox Signaling: https://www.liebertpub.com/doi/abs/10.1089/ars.2018.7707

Mancini, F. (1995, November 1). *Relative contributions of apolipoprotein(a) and apolipoprotein-B to the development of fatty lesions in the proximal aorta of mice*. Retrieved from Arteriosclerosis, Thrombosis and Vascular Biology: https://www.ahajournals.org/doi/full/10.1161/01.atv.15.11.1911

Manrique, C. (2013, October 1). *Obesity and Insulin Resistance Induce Early Development of Diastolic Dysfunction in Young Female Mice Fed a Western Diet*. Retrieved from Endocrinology: https://www.researchgate.net/publication/251878862_Obesity_and_Insulin_Resistance_Induce_Early_Development_of_Diastolic_Dysfunction_in_Young_Female_Mice_Fed_a_Western_Diet

Marcinova, S. (2002, August 2). *A critical evaluation of the role of Lp(a) in cardiovascular disease: can Lp(a) be useful in risk assessment?* Retrieved from Seminars in Vascular Medicine: https://www.thieme-connect.com/products/ejournals/abstract/10.1055/s-2002-35404

Marwick. (15. Jan 2018). *Implications of Underlying Mechanisms for the Recognition and Management of Diabetic Cardiomyopathy*. Von Journal of American College of Cardiology: https://www.jacc.org/doi/full/10.1016/j.jacc.2017.11.019 abgerufen

Maurya, S. (2023, April 8). *Ejection Fraction and Metabolic Shifts After Diastolic Dysfunction and Novel Cardiac Lipid Derangements*. Retrieved from Journals of American college of Cradiology: https://www.jacc.org/doi/10.1016/j.jacbts.2022.10.009

Mazumber, P., & Dale, A. (2004, September 1). *Impaired Cardiac Efficiency and Increased Fatty Acid Oxidation in Insulin-Resistant ob/ob Mouse Hearts*. Retrieved from Diabetes Journals: https://diabetesjournals.org/diabetes/article/53/9/2366/14717/Impaired-Cardiac-Efficiency-and-Increased-Fatty

McCormack. (2000, June 24). *Seeing what you want to see in randomised controlled trials: versions and perversions of UKPDS data*. Retrieved from British Medical Journal: https://www.bmj.com/content/320/7251/1720/rapid-responses

McDonagh. (2023, October 1). *2023 Focused Update of the 2021 ESC Guidelines for the diagnosis and treatment of acute and chronic heart failure: Developed by the task force for the diagnosis and treatment of acute and chronic heart failure of the European Society of Cardiology (ESC) W*. Retrieved from European Heart Journal: https://academic.oup.com/eurheartj/article/44/37/3627/7246292?login=false#427425189

McGavock. (2007, August 13). *Cardiac steatosis in diabetes mellitus: a 1H-magnetic resonance spectroscopy study*. Retrieved from Circulation: https://www.ahajournals.org/doi/10.1161/circulationaha.106.645614

McMillen, T. (2013, June 24). *Atherosclerosis and cardiac function assessment in low-density lipoprotein receptor-deficient mice undergoing body weight cycling*. Retrieved from Nature: https://www.nature.com/articles/nutd201319

McMurray. (6. September 2003). *Effects of candesartan in patients with chronic heart failure and reduced left-ventricular systolic function taking angiotensin-converting-enzyme inhibitors: the CHARM-Added trial*. Von The Lancet: https://www.thelancet.com/journals/lancet/article/PIIS0140-6736(03)14283-3/fulltext abgerufen

Miki. (2013, March 18). *Diabetic cardiomyopathy: pathophysiology and clinical features*. Retrieved from Heart Failure Reviews: https://pubmed.ncbi.nlm.nih.gov/22453289/

Mishra, P. (2013, December). *Cardiac matrix: a clue for future therapy*. Retrieved from Molecular Basis of Disease: https://www.sciencedirect.com/science/article/pii/S0925443913002834

Mori, J. (3. January 2014). *Angiotensin 1–7 Ameliorates Diabetic Cardiomyopathy and Diastolic Dysfunction in db/db Mice by Reducing Lipotoxicity and Inflammation*. Von Circulation: Heart Failure: https://www.ahajournals.org/doi/full/10.1161/CIRCHEARTFAILURE.113.000672#F1 abgerufen

Murdoch, Z. C. (2006, March 27). *Cardiovasc. Research.* Retrieved from https://pubmed.ncbi.nlm.nih.gov/16631149/

Murtaza, V. K. (2019). *Progress in Cardiovascular Disease*. Retrieved from https://www.sciencedirect.com/science/article/abs/pii/S0033062019300519

Muzzin, P. (1996, December 10). *Correction of obesity and diabetes in genetically obese mice by leptin gene therapy*. Retrieved from Proceedings of the National Academy of Sciences: https://www.pnas.org/doi/abs/10.1073/pnas.93.25.14804?doi=10.1073/pnas.93.25.14804

Nagueh, S. A. (2016). *Journal of the American Society of Echocardiography*. Retrieved from https://www.onlinejase.com/article/S0894-7317(16)00044-4/fulltext#secsectitle0040

Neuenschwander, M. (2019, July 3). *Role of diet in type 2 diabetes incidence: umbrella review of meta-analyses of prospective observational studies*. Retrieved from The British Journal of Medicine: https://www.bmj.com/content/366/bmj.l2368

Nevers, T. (2015, July 15). *Left Ventricular T-Cell Recruitment Contributes to the Pathogenesis of Heart Failure*. Retrieved from Circulation Heart Gailure: https://www.ahajournals.org/doi/10.1161/circheartfailure.115.002225

Neves, F. (2014, January). *Heart energy metabolism impairment in Western-diet induced obese mice*. Retrieved from The Journal of Nutritional Biochemistry: https://www.sciencedirect.com/science/article/abs/pii/S0955286313001964

Nguyen, S. (2017, August). *The effects of fatty acid composition on cardiac hypertrophy and function in mouse models of diet-induced obesity*. Retrieved from The Journal of Nutritional Biochemistry: https://www.sciencedirect.com/science/article/pii/S0955286317301286

Ni - Huping, S., & Dale, A. (2010, September 13). *PPARγ-induced cardiolipotoxicity in mice is ameliorated by PPARα deficiency despite increases in fatty acid oxidation*. Retrieved from Journal of Clinical Investigation: https://www.jci.org/articles/view/40905/sd/1

Nishikawa, T. (2000, April 13). *Normalizing mitochondrial superoxide production blocks three pathways of hyperglycaemic damage*. Retrieved from Nature: https://www.nature.com/articles/35008121

No authors listed. (1995, May 1). *Effect of intensive diabetes management on macrovascular events and risk factors in the Diabetes Control and Complications Trial*. Retrieved from The American Journal of Cardiology: Effect of intensive diabetes management on macrovascular events and risk factors in the Diabetes Control and Complications Trial

O'Brien, P. (2015, January 1). *BTBR ob/ob mice as a novel diabetic neuropathy model: neurological characterization and gene expression analyses*. Retrieved from Neurobiology of Disease: https://www.sciencedirect.com/science/article/abs/pii/S0969996114003283

Oka S, B. J. (2021, April 30). *Circulation Research.* Retrieved from https://www.ahajournals.org/doi/full/10.1161/CIRCRESAHA.120.317943

Oka, B. (2021, April 30). *American Heart Journals*. Retrieved from Nampt Potentiates Antioxidant Defense in Diabetic Cardiomyopathy: https://www.ahajournals.org/doi/10.1161/CIRCRESAHA.120.317943?url_ver=Z39.88-2003&rfr_id=ori:rid:crossref.org&rfr_dat=cr_pub%20%200pubmed

Oktay. (2020, August 1). *www.endotext.org.* Retrieved from https://www.ncbi.nlm.nih.gov/books/NBK560257/

Packer. (2001, May 31). *Effect of Carvedilol on Survival in Severe Chronic Heart Failure*. Retrieved from The New England Journal of Medicine: https://www.nejm.org/doi/full/10.1056/nejm200105313442201

Paigen, B. (1985, October). *Variation in susceptibility to atherosclerosis among inbred strains of mice*. Retrieved from Atherosclerosis: https://www.sciencedirect.com/science/article/abs/pii/0021915085901388

Quang, K. (2014, August 14). *Early Development of Calcific Aortic Valve Disease and Left Ventricular Hypertrophy in a Mouse Model of Combined Dyslipidemia and Type 2 Diabetes Mellitus* . Retrieved from Ateriosclerosis, Thrombosis and Vascular Biology: https://www.ahajournals.org/doi/full/10.1161/ATVBAHA.114.304205

Ramesh, P. (2022, March 15). *The role of inflammation in diabetic cardiomyopathy*. Retrieved from Therapeutic Advacnes in Endocrinology and Metabolism: https://journals.sagepub.com/doi/full/10.1177/20420188221083530

Rashid, S. (2005, April 1). *Decreased plasma cholesterol and hypersensitivity to statins in mice lacking Pcsk9*. Retrieved from The Proceedings of the National Academy of Sciences: https://www.pnas.org/doi/full/10.1073/pnas.0501652102

Rigotti, A. (1997, November 11). *A targeted mutation in the murine gene encoding the high density lipoprotein (HDL) receptor scavenger receptor class B type I reveals its key role in HDL metabolism*. Retrieved from The Proceedings of the National Academy of Sciences: https://www.pnas.org/doi/full/10.1073/pnas.94.23.12610

Ritchie, & Dale. (2020, May 21). *Circulation Research.* Retrieved from https://doi.org/10.1161/CIRCRESAHA.120.315913

Rubler. (1972, November 8). *New type of cardiomyopathy associated with diabetic glomerulosclerosis*. Retrieved from American Journal of Cardiology: https://www.ajconline.org/article/0002-9149(72)90595-4/fulltext

Sadhukan. (2016, April 5). *Metabolomics-assisted proteomics identifies succinylation and SIRT5 as important regulators of cardiac function.* Retrieved from https://www.pnas.org/doi/full/10.1073/pnas.1519858113

Seferovic, P. (2015, April 17). *European Heart Journal.* Retrieved from https://academic.oup.com/eurheartj/article/36/27/1718/2398074?login=false

Segar, M., Khan, M., & Patel K, B. J. (2021). *Journals of American College of Cardiology*. Retrieved from https://www.jacc.org/doi/10.1016/j.jacc.2021.08.020

Seidah, N. (2022, June 3). *The Multifaceted Biology of PCSK9*. Retrieved from endocrine reviews: https://academic.oup.com/edrv/article/43/3/558/6385885

Sharma, K. (2003, June 1). *Diabetic kidney disease in the db/db mouse*. Retrieved from American Journal of Renal Physiology: https://journals.physiology.org/doi/full/10.1152/ajprenal.00315.2002

Smith. (31. Ocotber 2003). *The emergence of mouse models of atherosclerosis and their relevance to clinical research*. Von Journal of Internal Medicine: https://onlinelibrary.wiley.com/doi/abs/10.1046/j.1365-2796.1997.00197.x?sid=nlm%3Apubmed abgerufen

Smith, C. (2011, April 21). *Epicardial-Derived Cell Epithelial-to-Mesenchymal Transition and Fate Specification Require PDGF Receptor Signaling*. Retrieved from Circulation Research: https://www.ahajournals.org/doi/10.1161/circresaha.110.235531

Sorop, O. (2018, June 1). *Multiple common comorbidities produce left ventricular diastolic dysfunction associated with coronary microvascular dysfunction, oxidative stress, and myocardial stiffening*. Retrieved from Cardiovascular Research: https://academic.oup.com/cardiovascres/article/114/7/954/4844872

Souders, C. (2009, December 4). *Cardiac fibroblast: the renaissance cell*. Retrieved from Circulation: https://www.ahajournals.org/doi/10.1161/CIRCRESAHA.109.209809

Srinivasan, K. (2007, February 13). *Animal models in type 2 diabetes research: an overview*. Retrieved from The Indian Journal of Medical Research: https://www.researchgate.net/publication/6336329_Animal_models_in_type_2_diabetes_research_An_overview_K

Stewart, J., Addy, K., & Campbell, S. (2020, August 26). *JRSM Cardiovascular Disease.* Retrieved from https://www.ncbi.nlm.nih.gov/pmc/articles/PMC7502686/

Sullivan, M. (15. July 2015). *Impairment of Liver Glycogen Storage in the db/db Animal Model of Type 2 Diabetes: A Potential Target for Future Therapeutics?* Von Current Drug targets: https://pubmed.ncbi.nlm.nih.gov/26212261/ abgerufen

Suriano. (2021, June 28). *Novel insights into the genetically obese (ob/ob) and diabetic (db/db) mice: two sides of the same coin*. Retrieved from Microbiome Journal: https://microbiomejournal.biomedcentral.com/articles/10.1186/s40168-021-01097-8

Tadinada, S. (2021, October 11). *Functional resilience of C57BL/6J mouse heart to dietary fat overload*. Retrieved from American Journal of Physiology: https://journals.physiology.org/doi/full/10.1152/ajpheart.00419.2021

Takeshi, A. (1999, January 22). *Decreased Atherosclerosis in Heterozygous Low Density Lipoprotein Receptor-deficient Mice Expressing the Scavenger Receptor BI Transgene*. Retrieved from Journal of Biological Chemistry: https://www.sciencedirect.com/science/article/pii/S0021925819881863

Tan, Y. (2011, February). *Diabetic downregulation of Nrf2 activity via ERK contributes to oxidative stress-induced insulin resistance in cardiac cells in vitro and in vivo*. Retrieved from Diabetes: https://watermark.silverchair.com/625.pdf?token=AQECAHi208BE49Ooan9kkhW_Ercy7Dm3ZL_9Cf3qfKAc485ysgAAAy4wggMqBgkqhkiG9w0BBwagggMbMIIDFwIBADCCAxAGCSqGSIb3DQEHATAeBglghkgBZQMEAS4wEQQMcseUvq4D65isVXcSAgEQgIIC4biOmQcVuGSRLoVXZb4yDKAtRE2n52P23wY9brDdNAlX0ZVySSD

Tan, Y. (2020, February 20). *Nature Reviews Cardiology.* Retrieved from https://www.nature.com/articles/s41569-020-0339-2

Tang, M. (2021, March 15). *Stiffness of aortic arch and carotid arteries increases in ApoE-knockout mice with high-fat diet: evidence from echocardiography*. Retrieved from American Journal of Translational Sciences: https://www.researchgate.net/publication/350846831_Stiffness_of_aortic_arch_and_carotid_arteries_increases_in_ApoE-knockout_mice_with_high-fat_diet_evidence_from_echocardiography

Tang, Z. (2017, April 13). *New role of PCSK9 in atherosclerotic inflammation promotion involving the TLR4/NF-κB pathway*. Retrieved from Atherosclerosis: https://www.sciencedirect.com/science/article/abs/pii/S0021915017301879

Tannous, B. (27. August 2020). *Acta Physiologica*. Von Nicotinamide adenine dinucleotide: Biosynthesis, consumption and therapeutic role in cardiac diseases: https://onlinelibrary.wiley.com/doi/10.1111/apha.13551 abgerufen

Tesch, G. (2011, February 1). *Recent insights into diabetic renal injury from the db/db mouse model of type 2 diabetic nephropathy*. Retrieved from American Journals of Physiology: https://journals.physiology.org/doi/full/10.1152/ajprenal.00607.2010

Tikellis, C. (2008, May 13). *Cardiac inflammation associated with a Western diet is mediated via activation of RAGE by AGEs*. Retrieved from American Journal of Physiology: https://pubmed.ncbi.nlm.nih.gov/18477705/

Toffoli, B. (2011, 04 January). *TRAIL shows potential cardioprotective activity*. Retrieved from Investigational New Drugs: https://europepmc.org/article/med/21197620

Torikai, H. (2023, March 2). *Atherogenesis in Apoe−/− and Ldlr−/− Mice with a Genetically Resistant Background*. Retrieved from Cells: https://www.mdpi.com/2073-4409/12/9/1255/review_report

Travers, J. (2016, March 16). *Cardiac Fibrosis: The Fibroblast Awakens*. Retrieved from Circulation Research: https://www.ahajournals.org/doi/full/10.1161/CIRCRESAHA.115.306565

Tse. (2004, 16 August). *Accelerated atherosclerosis and premature calcified cartilaginous metaplasia in the aorta of diabetic male Apo E knockout mice can be prevented by chronic treatment with 17 beta-estradiol*. Retrieved from Atherosclerosis: https://www.atherosclerosis-journal.com/article/S0021-9150(98)00325-6/abstract

UKPDS, U. P. (12. September 1998). *The Lancet.* Von The Lancet: https://www.thelancet.com/journals/lancet/article/PIIS0140-6736(98)07019-6/fulltext abgerufen

Van Linthout, S. (2008, March 18). *Reduced MMP-2 activity contributes to cardiac fibrosis in experimental diabetic cardiomyopathy*. Retrieved from Basic Research Cardiology: https://link.springer.com/article/10.1007/s00395-008-0715-2

Veniant, M. (2001, October 1). *Lipoprotein Size and Atherosclerosis Susceptibility in Apoe−/− and Ldlr−/− Mice*. Retrieved from AHA Journals: https://www.ahajournals.org/doi/full/10.1161/hq1001.097780#:~:text=The%20finding%20of%20substantially%20more,B%2D100–containing%20lipoproteins.

Wang, D. (2023, February 8). *Hepatic Nampt Deficiency Aggravates Dyslipidemia and Fatty Liver in High Fat Diet Fed Mice*. Retrieved from Cells: https://www.mdpi.com/2073-4409/12/4/568

Wang, Q. (2016, November 4). *Inhibiting Insulin-Mediated β2-Adrenergic Receptor Activation Prevents Diabetes-Associated Cardiac Dysfunction*. Retrieved from Circulation: https://www.ahajournals.org/doi/full/10.1161/CIRCULATIONAHA.116.022281

Weixin. (2016, April 18). *EGFR Inhibition Blocks Palmitic Acid-induced inflammation in cardiomyocytes and Prevents Hyperlipidemia-induced Cardiac Injury in Mice*. Retrieved from Nature: https://www.nature.com/articles/srep24580

Wilson, A. (2018, February 10). *Reactive oxygen species signalling in the diabetic heart: emerging prospect for therapeutic targeting*. Retrieved from British Journal of Medicine Heart: https://heart.bmj.com/content/104/4/293

Wing. (2013, July 11). *Cardiovascular Effects of Intensive Lifestyle Intervention in Type 2 Diabetes*. Retrieved from The New England Journal of Medicine: https://www.nejm.org/doi/full/10.1056/nejmoa1212914

Wiviott. (2019, January 24). *Dapaglifozin and Cardiovascular Outcomes in Type 2 Diabetes*. Retrieved from The New England Journal of Medicine: https://www.nejm.org/doi/full/10.1056/nejmoa1812389

Wright, J. (2009, May 1). *Mechanisms for increased myocardial fatty acid utilization following short-term high-fat feeding*. Retrieved from Cardiovascular Research: https://academic.oup.com/cardiovascres/article/82/2/351/278389

Xiaoquing. (1. November 2008). *Nrf2 is critical in defense against high glucose-induced oxidative damage in cardiomyocytes*. Von Journal of Molecular and Cellular Cardiology: https://europepmc.org/article/med/19007787 abgerufen

Xin, Y. (2018, January 2). *Sulforaphane prevents angiotensin II-induced cardiomyopathy by activation of Nrf2 via stimulating the Akt/GSK-3ß/Fyn pathway*. Retrieved from Redox Biology: https://www.sciencedirect.com/science/article/pii/S2213231717308649

Yan, M. (2022, May 11). *Mitochondrial damage and activation of the cytosolic DNA sensor cGAS–STING pathway lead to cardiac pyroptosis and hypertrophy in diabetic*

cardiomyopathy mice. Retrieved from Nature: https://www.nature.com/articles/s41420-022-01046-w

Yang. (2019, March 11). *Gut Microbiota Composition and Structure of the Ob/Ob and Db/Db Mice*. Retrieved from International Journal of Endocrinology: https://www.hindawi.com/journals/ije/2019/1394097/

Yoshino. (2011, October 5). *Nicotinamide Mononucleotide, a Key NAD+ Intermediate, Treats the Pathophysiology of Diet- and Age-Induced Diabetes in Mice.* Retrieved from Cell Metabolism: https://www.cell.com/cell-metabolism/fulltext/S1550-4131(11)00346-9?_returnURL=https%3A%2F%2Flinkinghub.elsevier.com%2Fretrieve%2Fpii%2FS1550413111003469%3Fshowall%3Dtrue

Yoshino. (2021, June 11). *Science.* Retrieved from Nicotinamide mononucleotide increases muscle insulin sensitivity in prediabetic women: https://www.science.org/doi/10.1126/science.abe9985

Yusuf. (2001, October 17). *Ramipril and the Development of Diabetes*. Retrieved from Journal of the American Medical Association: https://jamanetwork.com/journals/jama/fullarticle/194283

Zaid. (2008, April 11). *Proprotein convertase subtilisin/kexin type 9 (PCSK9): hepatocyte-specific low-density lipoprotein receptor degradation and critical role in mouse liver regeneration*. Retrieved from Hepatology: https://europepmc.org/article/med/18666258

Zaragoza. (2011, February 2011). *Animal models of cardiovascular diseases*. Retrieved from Journal of Biomedical Biotechnology: https://www.hindawi.com/journals/bmri/2011/497841/

Zhang, H. (2022, April 22). *Quantification of Early Diffuse Myocardial Fibrosis Through 7.0 T Cardiac Magnetic Resonance T1 Mapping in a Type 1 Diabetic Mellitus Mouse Model*. Retrieved from Journals of Magnetic Resonance Imaging: https://onlinelibrary.wiley.com/doi/10.1002/jmri.28207

Zhang, L. (2010, August 10). *Cardiac diacylglycerol accumulation in high fat-fed mice is associated with impaired insulin-stimulated glucose oxidation*. Retrieved from Cardiovascular Research: https://academic.oup.com/cardiovascres/article/89/1/148/325403

Zhang, S. (1992, Ocotber 16). *Spontaneous hypercholesterolemia and arterial lesions in mice lacking apolipoprotein E*. Retrieved from Science: https://www.science.org/doi/10.1126/science.1411543

Zhao, Y. (2020, June 20). *Small rodent models of atherosclerosis*. Retrieved from Biomedicine & Pharmacotherapy: https://www.sciencedirect.com/science/article/pii/S0753332220306193

Zinman B, W. C. (2015, November 26). *New England Journal of Medicine.* Retrieved from https://www.nejm.org/doi/full/10.1056/nejmoa1504720